
Riemannian stochastic variance reduced gradient on Grassmann manifold

Hiroyuki Kasai

The University of Electro-Communications
Tokyo, Japan
kasai@is.uec.ac.jp

Hiroyuki Sato

Tokyo University of Science
Tokyo, Japan
hsato@rs.tus.ac.jp

Bamdev Mishra

Amazon Development Centre India,
Bangalore, India
bamdevm@amazon.com

Abstract

Stochastic variance reduction algorithms have recently become popular for minimizing the average of a large, but finite, number of loss functions. In this paper, we propose a novel Riemannian extension of the Euclidean stochastic variance reduced gradient algorithm (R-SVRG) to a compact manifold search space. To this end, we show the developments on the Grassmann manifold. The key challenges of averaging, addition, and subtraction of multiple gradients are addressed with notions like logarithm mapping and parallel translation of vectors on the Grassmann manifold. We present a global convergence analysis of the proposed algorithm with decaying step-sizes and a local convergence rate analysis under fixed step-size with some natural assumptions. The proposed algorithm is applied on a number of problems on the Grassmann manifold like principal components analysis, low-rank matrix completion, and the Karcher mean computation. In all these cases, the proposed algorithm outperforms the standard Riemannian stochastic gradient descent algorithm.

1 Introduction

A general loss minimization problem is defined as $\min_w f(w)$, where $f(w) := \frac{1}{N} \sum_{n=1}^N f_n(w)$, w is the model variable, N is the number of samples, and $f_n(w)$ is the loss incurred on n -th sample. The *full gradient decent* (GD) algorithm requires evaluations of N derivatives, i.e., $\sum_{n=1}^N \nabla f_n(w)$, per iteration, which is computationally heavy when N is very large. A popular alternative is to use only one derivative $\nabla f_n(w)$ per iteration for n -th sample, which is the basis of the *stochastic gradient descent* (SGD) algorithm. When a relatively large step-size is used in SGD, the train loss decreases fast in the beginning, but results in big fluctuations around the solution. On the other hand, when a small step-size is used, SGD requires a large number of iterations to converge. To circumvent this issue, SGD starts with a relatively large step-size and decreases it gradually with iterations.

Recently, *variance reduction* techniques have been proposed to accelerate the convergence of SGD [1, 2, 3, 4, 5, 6, 7]. Stochastic variance reduced gradient (SVRG) is a popular algorithm that enjoys superior convergence properties [1]. For smooth and strongly convex functions, SVRG has convergence rates similar to those of stochastic dual coordinate ascent [5] and stochastic average gradient (SAG) algorithms [3]. Garber and Hazan [8] analyze the convergence rate for SVRG when f is a convex function that is a sum of non-convex (but smooth) terms and apply this result to the principal component analysis (PCA) problem. Shalev-Shwartz [9] also proposes similar results. Allen-Zhu

and Yuan [10] further study the same case with better convergence rates. Shamir [11] studies specifically the convergence properties of the variance reduction PCA algorithm. Very recently, Allen-Zhu and Hazan [12] propose a variance reduction method for faster non-convex optimization. However, it should be noted that all these cases assume that search space is Euclidean.

In this paper, we deal with problems where the variables have a manifold structure. They include, for example, the low-rank matrix completion problem [13], the Karcher mean computation problem, and the PCA problem. In all these problems, optimization on *Riemannian manifolds* has shown state-of-the-art performance. The Riemannian framework exploits the geometry of the constrained matrix search space to design efficient optimization algorithms [14]. Specifically, the problem $\min_{w \in \mathcal{M}} f(w)$, where \mathcal{M} is a Riemannian manifold, is solved as an *unconstrained optimization problem* defined over the Riemannian manifold search space. Bonnabel [15] proposes a *Riemannian stochastic gradient* algorithm (R-SGD) that extends SGD from the Euclidean space to Riemannian manifolds.

Building upon the work of Bonnabel [15], we propose a novel (and to the best of our knowledge, the first) extension of the stochastic variance reduction gradient algorithm in the Euclidean space to the Riemannian manifold search space (R-SVRG). This extension is not trivial and requires particular consideration in dealing with averaging, addition and subtraction of multiple gradients at different points on the manifold \mathcal{M} . To this end, this paper specifically focuses on the *Grassmann manifold* $\text{Gr}(r, d)$, which is the set of r -dimensional linear subspaces in \mathbb{R}^d . Nonetheless, the proposed algorithm and the analysis presented in this paper can be generalized to other compact Riemannian manifolds.

The paper is organized as follows. Section 2 discusses the Grassmann manifold and three popular optimization problems, where the Grassmann manifold plays an essential role. The detailed description of R-SVRG are given in Section 3. Section 4 presents the global convergence analysis and the local convergence rate analysis of R-SVRG. In Section 5, numerical comparisons with R-SGD on the three problems suggest superior performance of R-SVRG. The brief explanation of optimization on manifold is introduced in Section A of the supplementary material file. The concrete proofs of the main theorems and the related lemmas, and additional numerical experiments are shown in Sections B, C, and D, respectively, of the supplementary file. Our proposed R-SVRG is implemented in the Matlab toolbox Manopt [16]. The Matlab codes for the proposed algorithms are available at <https://bamdevmishra.com/codes/RSVRG/>.

2 Grassmann manifold and problems on Grassmann manifold

This section briefly introduces the Grassmann manifold and motivates three problems on the Grassmann manifold.

Grassmann manifold. An element on the Grassmann manifold is represented by a $d \times r$ orthogonal matrix \mathbf{U} with orthonormal columns, i.e., $\mathbf{U}^T \mathbf{U} = \mathbf{I}$. Two orthogonal matrices represent the same element on the Grassmann manifold if they are related by right multiplication of a $r \times r$ orthogonal matrix $\mathbf{O} \in \mathcal{O}(r)$. Equivalently, an element of the Grassmann manifold is identified with a set of $d \times r$ orthogonal matrices $[\mathbf{U}] := \{\mathbf{U}\mathbf{O}_r : \mathbf{O}_r \in \mathcal{O}(r)\}$. In other words, $\text{Gr}(r, d) := \text{St}(r, d)/\mathcal{O}(r)$, where $\text{St}(r, d)$ is the *Stiefel manifold* that is the set of matrices of size $d \times r$ with orthonormal columns. The Grassmann manifold has the structure of a Riemannian quotient manifold [14, Section 3.4].

Geodesics on manifolds generalize the concept of straight lines in the Euclidean space. For every vector in the tangent space $\xi \in T_w \mathcal{M}$ at $w \in \mathcal{M}$, there exists an interval I about 0 and a unique geodesic $\gamma_e(t, w, \xi) : I \rightarrow \mathcal{M}$ such that $\gamma_e(0) = w$ and $\dot{\gamma}_e(0) = \xi$. The mapping $\text{Exp}_w : T_w \mathcal{M} \rightarrow \mathcal{M} : \xi \mapsto \text{Exp}_w \xi = \gamma_e(1, w, \xi)$ is called the *exponential mapping* at w . If \mathcal{M} is a complete manifold, exponential mapping is defined for all vectors $\xi \in T_w \mathcal{M}$. The exponential mapping for the Grassmann manifold from $\mathbf{U}(0) := \mathbf{U} \in \text{Gr}(r, d)$ in the direction of $\xi \in T_{\mathbf{U}(0)}$ is given in closed form as [14, Section 5.4]

$$\mathbf{U}(t) = [\mathbf{U}(0)\mathbf{V} \ \mathbf{W}] \begin{bmatrix} \cos t\Sigma \\ \sin t\Sigma \end{bmatrix} \mathbf{V}^T, \quad (1)$$

where $\xi = \mathbf{W}\Sigma\mathbf{V}^T$ is the rank- r singular value decomposition of ξ . The $\cos(\cdot)$ and $\sin(\cdot)$ operations are only on the diagonal entries.

Parallel translation transports a vector field along the geodesic curve γ that satisfies $P_\gamma^{a \leftarrow a} = \gamma(a)$ and $\frac{D}{dt}(P_\gamma^{t \leftarrow a} \xi(a)) = 0$ [14, Section 5.4], where $P_\gamma^{b \leftarrow a}$ is the parallel translation operator sending $\xi(a)$ to $\xi(b)$. The parallel translation of $\zeta \in T_{\mathbf{U}(0)}$ on the Grassmann manifold along $\gamma(t)$ with ξ is given in closed form by

$$\zeta(t) = \left([\mathbf{U}(0)\mathbf{V} \ \mathbf{W}] \begin{bmatrix} -\sin t\Sigma \\ \cos t\Sigma \end{bmatrix} \mathbf{W}^T + (\mathbf{I} - \mathbf{W}\mathbf{W}^T) \right) \zeta. \quad (2)$$

Given two points w and z on \mathcal{M} , the *logarithm mapping* or simply *log mapping* maps z to a vector $\xi \in T_w\mathcal{M}$ on the tangent space at w . Specifically, it is defined by $\text{Log}_w : \mathcal{M} \rightarrow T_w\mathcal{M} : \text{Exp}_w \xi \mapsto \text{Log}_w(\text{Exp}_w \xi) = \xi$. It should be noted that it satisfies $\text{dist}(w, z) = \|\text{Log}_w(z)\|_w$, where $\text{dist} : \mathcal{M} \times \mathcal{M} \rightarrow \mathbb{R}$ is the *shortest* distance between w and z . The logarithm map of $\mathbf{U}(t)$ at $\mathbf{U}(0)$ on the Grassmann manifold is given by

$$\xi = \log_{\mathbf{U}(0)}(\mathbf{U}(t)) = \mathbf{W} \arctan(\Sigma) \mathbf{V}^T, \quad (3)$$

where $\mathbf{W}\Sigma\mathbf{V}^T$ is the rank- r singular value decomposition of $(\mathbf{U}(t) - \mathbf{U}(0)\mathbf{U}(0)^T\mathbf{U}(t))(\mathbf{U}(0)^T\mathbf{U}(t))^{-1}$.

Problems on Grassmann manifold. In this paper, we focus on three popular problems on the Grassmann manifold, which are the PCA, low-rank matrix completion, and the Karcher mean computation problems. In all these problems, full gradient methods, e.g., the steepest descent algorithm, become prohibitively computationally expensive when N is very large, and the stochastic gradient approach is one promising way to achieve scalability.

Given an orthonormal matrix projector $\mathbf{U} \in \text{St}(r, d)$, the PCA problem is to minimize the sum of squared residual errors between projected data points and the original data as

$$\min_{\mathbf{U} \in \text{St}(r, d)} \frac{1}{N} \sum_{n=1}^N \|\mathbf{x}_n - \mathbf{U}\mathbf{U}^T \mathbf{x}_n\|_2^2, \quad (4)$$

where \mathbf{x}_n is a data vector of size $d \times 1$. The problem (4) is equivalent to maximizing $\frac{1}{N} \sum_{n=1}^N \mathbf{x}_n^T \mathbf{U}\mathbf{U}^T \mathbf{x}_n$. Here, the critical points in the space $\text{St}(r, d)$ are not isolated because the cost function remains unchanged under the group action $\mathbf{U} \mapsto \mathbf{U}\mathbf{O}$ for all orthogonal matrices \mathbf{O} of size $r \times r$. Subsequently, the problem (4) is an optimization problem on the Grassmann manifold $\text{Gr}(r, d)$.

The Karcher mean is introduced as a notion of *mean* on Riemannian manifolds by Karcher [17]. It generalizes the notion of an “average” on the manifold. Given N points on the Grassmann manifold with matrix representations $\mathbf{Q}_1, \dots, \mathbf{Q}_N$, the Karcher mean is defined as the solution to the problem

$$\min_{\mathbf{U} \in \text{St}(r, d)} \frac{1}{2N} \sum_{n=1}^N (\text{dist}(\mathbf{U}, \mathbf{Q}_n))^2, \quad (5)$$

where dist is the geodesic distance between the elements on the Grassmann manifold. The gradient of this loss function is $\frac{1}{N} \sum_{n=1}^N -\text{Log}_{\mathbf{U}}(\mathbf{Q}_n)$, where Log is the log map defined in (3). The Karcher mean on the Grassmann manifold $\text{Gr}(r, d)$ is frequently used for computer vision problems such as visual object categorization and pose categorization [18]. Since recursive calculations of the Karcher mean are needed with each new arriving visual image, the stochastic gradient algorithm becomes an appealing choice for large datasets.

The matrix completion problem amounts to completing an incomplete matrix \mathbf{X} , say of size $d \times N$, from a small number of entries by assuming a low-rank model for the matrix. If Ω is the set of the indices for which we know the entries in \mathbf{X} , the rank- r matrix completion problem amounts to solving the problem

$$\min_{\mathbf{U} \in \mathbb{R}^{d \times r}, \mathbf{A} \in \mathbb{R}^{r \times N}} \|\mathcal{P}_\Omega(\mathbf{U}\mathbf{A}) - \mathcal{P}_\Omega(\mathbf{X})\|_F^2, \quad (6)$$

where the operator $\mathcal{P}_\Omega(\mathbf{X}_{ij}) = \mathbf{X}_{ij}$ if $(i, j) \in \Omega$ and $\mathcal{P}_\Omega(\mathbf{X}_{ij}) = 0$ otherwise is called the orthogonal sampling operator and is a mathematically convenient way to represent the subset of known entries. Partitioning $\mathbf{X} = [\mathbf{x}_1, \mathbf{x}_2, \dots, \mathbf{x}_N]$, the problem (6) is equivalent to the problem

$$\min_{\mathbf{U} \in \mathbb{R}^{d \times r}, \mathbf{a}_n \in \mathbb{R}^r} \frac{1}{N} \sum_{n=1}^N \|\mathcal{P}_{\Omega_n}(\mathbf{U}\mathbf{a}_n) - \mathcal{P}_{\Omega_n}(\mathbf{x}_n)\|_2^2, \quad (7)$$

where $\mathbf{x}_n \in \mathbb{R}^d$ and the operator \mathcal{P}_{Ω_n} the sampling operator for the n -th column. Given \mathbf{U} , \mathbf{a}_n in (7) admits a closed-form solution. Consequently, the problem (7) only depends on the column space of \mathbf{U} and is on the Grassmann manifold [19].

3 Riemannian stochastic variance reduced gradient on Grassmann manifold

After a brief explanation of the variance reduced gradient variants in the Euclidean space, the Riemannian stochastic variance reduced gradient on the Grassmann manifold is proposed.

Variance reduced gradient variants in the Euclidean space. The SGD update in the Euclidean space is $w_{t+1} = w_t - \eta v_t$, where v_t is a randomly selected vector that is called as the *stochastic gradient* and η is the step-size. SGD assumes an *unbiased estimator* of the full gradient as $\mathbb{E}_n[\nabla f_n(w_t)] = \nabla f(w_t)$. Many recent variants of the variance reduced gradient of SGD attempt to reduce its variance $\mathbb{E}[\|v_t - \nabla f(w_t)\|^2]$ as t increases to achieve better convergence [1, 2, 3, 4, 5, 6, 7]. SVRG, proposed in [1], introduces an explicit variance reduction strategy with double loops where s -th outer loop, called s -th *epoch*, has m_s inner iterations. SVRG first keeps $\tilde{w} = w_{m_s}^{s-1}$ or $\tilde{w} = w_t^{s-1}$ for randomly chosen $t \in \{1, \dots, m_{s-1}\}$ at the end of $(s-1)$ -th epoch, and also sets the initial value of s -th epoch as $w_0^s = \tilde{w}$. It then computes a full gradient $\nabla f(\tilde{w})$. Subsequently, denoting the selected random index $i \in \{1, \dots, N\}$ by i_t^s , SVRG randomly picks i_t^s -th sample for each $t \geq 1$ at $s \geq 1$ and computes the *modified stochastic gradient* v_t^s as

$$v_t^s = \nabla f_{i_t^s}(w_{t-1}^s) - \nabla f_{i_t^s}(\tilde{w}^{s-1}) + \nabla f(\tilde{w}^{s-1}). \quad (8)$$

It should be noted that SVRG can be regarded as one special case of S2GD (Semi-stochastic gradient descent), which differs in the number of inner loop iterations chosen [20].

Proposed Riemannian extension of SVRG on Grassmann manifold (R-SVRG). We propose a Riemannian extension of SVRG, i.e., R-SVRG. Here, we denote the Riemannian stochastic gradient for i_t^s -th sample as $\text{grad} f_{i_t^s}(\tilde{\mathbf{U}}^{s-1})$ and the *modified Riemannian stochastic gradient* as ξ_t^s instead of v_t^s to show differences with the Euclidean case.

The way R-SVRG reduces the variance is analogous to the SVRG algorithm in the Euclidean case. More specifically, R-SVRG keeps a $\tilde{\mathbf{U}}^{s-1} \in \mathcal{M} = \text{Gr}(r, d)$ after m_{s-1} stochastic update steps of $(s-1)$ -th epoch, and computes the full Riemannian gradient $\text{grad} f(\tilde{\mathbf{U}}^{s-1}) = \frac{1}{N} \sum_{i=1}^N \text{grad} f_i(\tilde{\mathbf{U}}^{s-1})$ only for this stored $\tilde{\mathbf{U}}^{s-1}$. The algorithm also computes the Riemannian stochastic gradient $\text{grad} f_{i_t^s}(\tilde{\mathbf{U}}^{s-1})$ that corresponds to this i_t^s -th sample. Then, picking i_t^s -th sample for each t -th inner iteration of s -th epoch at \mathbf{U}_{t-1}^s , we calculate ξ_t^s in the same way as v_t^s in (8), i.e., by modifying the stochastic gradient $\text{grad} f_{i_t^s}(\mathbf{U}_{t-1}^s)$ using both $\text{grad} f(\tilde{\mathbf{U}}^{s-1})$ and $\text{grad} f_{i_t^s}(\tilde{\mathbf{U}}^{s-1})$. Translating the right-hand side of (8) to the manifold \mathcal{M} involves the sum of $\text{grad} f_{i_t^s}(\mathbf{U}_{t-1}^s)$, $\text{grad} f_{i_t^s}(\tilde{\mathbf{U}}^{s-1})$, and $\text{grad} f(\tilde{\mathbf{U}}^{s-1})$, which belong to two separate tangent spaces $T_{\mathbf{U}_{t-1}^s} \mathcal{M}$ and $T_{\tilde{\mathbf{U}}^{s-1}} \mathcal{M}$. This operation requires particular attention on a manifold and parallel translation provides an adequate and flexible solution to handle multiple elements on two separated tangent spaces. More concretely, $\text{grad} f_{i_t^s}(\tilde{\mathbf{U}}^{s-1})$ and $\text{grad} f(\tilde{\mathbf{U}}^{s-1})$ are firstly parallel-transported to $T_{\mathbf{U}_{t-1}^s} \mathcal{M}$ at the current point \mathbf{U}_{t-1}^s , then they are ready to be added to $\text{grad} f_{i_t^s}(\mathbf{U}_{t-1}^s)$ on $T_{\mathbf{U}_{t-1}^s} \mathcal{M}$. Consequently, the modified Riemannian stochastic gradient ξ_t^s at t -th inner iteration of s -th epoch is set as

$$\xi_t^s = \text{grad} f_{i_t^s}(\mathbf{U}_{t-1}^s) - P_{\gamma}^{\mathbf{U}_{t-1}^s \leftarrow \tilde{\mathbf{U}}^{s-1}} \left(\text{grad} f_{i_t^s}(\tilde{\mathbf{U}}^{s-1}) \right) + P_{\gamma}^{\mathbf{U}_{t-1}^s \leftarrow \tilde{\mathbf{U}}^{s-1}} \left(\text{grad} f(\tilde{\mathbf{U}}^{s-1}) \right), \quad (9)$$

where $P_{\gamma}^{\mathbf{U}_{t-1}^s \leftarrow \tilde{\mathbf{U}}^{s-1}}(\cdot)$ represents a parallel-translation operator from $\tilde{\mathbf{U}}^{s-1}$ to \mathbf{U}_{t-1}^s on the Grassmann manifold defined in (2). Furthermore, for this parallel translation, we need to calculate the tangent vector from $\tilde{\mathbf{U}}^{s-1}$ to \mathbf{U}_{t-1}^s . This is given by the logarithm mapping defined in (3). Consequently, the final update rule of R-SVRG is defined as $\mathbf{U}_t^s = \text{Exp}_{\mathbf{U}_{t-1}^s}(-\eta \xi_t^s)$. It should be noted that the modified direction ξ_t^s is also a Riemannian stochastic gradient of f at \mathbf{U}_{t-1}^s .

Conditioned on \mathbf{U}_{t-1}^s , we take the expectation with respect to i_t^s and obtain

$$\begin{aligned}\mathbb{E}_{i_t^s}[\xi_t^s] &= \mathbb{E}_{i_t^s}[\text{grad}f_{i_t^s}(\mathbf{U}_{t-1}^s)] - P_{\gamma}^{\mathbf{U}_{t-1}^s \leftarrow \tilde{\mathbf{U}}^{s-1}} \left(\mathbb{E}_{i_t^s}[\text{grad}f_{i_t^s}(\tilde{\mathbf{U}}^{s-1})] - \text{grad}f(\tilde{\mathbf{U}}^{s-1}) \right) \\ &= \text{grad}f(\mathbf{U}_{t-1}^s) - P_{\gamma}^{\mathbf{U}_{t-1}^s \leftarrow \tilde{\mathbf{U}}^{s-1}} \left(\text{grad}f(\tilde{\mathbf{U}}^{s-1}) - \text{grad}f(\tilde{\mathbf{U}}^{s-1}) \right) \\ &= \text{grad}f(\mathbf{U}_{t-1}^s).\end{aligned}$$

The theoretical analysis of convergence of the Euclidean SVRG algorithm assumes that the beginning vector \mathbf{U}_0^s of s -th epoch is set to be the average (or a random) vector of the $(s-1)$ -th epoch [1, Figure 1]. However, the set of the last vector in the $(s-1)$ -th epoch, i.e., $\mathbf{U}_{m_{s-1}}^{s-1}$ shows the superior performances on the Euclidean SVRG algorithm. Therefore, for our local convergence rate analysis in **Theorem 4.3**, this paper also uses, as **option I**, the mean value of $\tilde{\mathbf{U}}^s = g_{m_s}(\mathbf{U}_1^s, \dots, \mathbf{U}_{m_s}^s)$ as $\tilde{\mathbf{U}}^s$, where $g_n(\mathbf{U}_1, \dots, \mathbf{U}_n)$ is the Karcher mean on the Grassmann manifold. This option can also simply choose $\tilde{\mathbf{U}}^s = \mathbf{U}_t^s$ for $t \in \{1, \dots, m_s\}$ at random. In addition, as **option II**, we can also use the last vector in the $(s-1)$ -th epoch, i.e., $\tilde{\mathbf{U}}^s = \mathbf{U}_{m_s}^{s-1}$. The overall algorithm with a fixed step-size is summarized in Algorithm 1.

Algorithm 1 Algorithm for R-SVRG with a fixed step-size.

Require: Update frequency $m_s > 0$ and step-size $\eta > 0$.

- 1: Initialize $\tilde{\mathbf{U}}^0$.
 - 2: **for** $s = 1, 2, \dots$ **do**
 - 3: Calculate the Riemannian full gradient $\text{grad}f(\tilde{\mathbf{U}}^{s-1})$.
 - 4: Store $\mathbf{U}_0^s = \tilde{\mathbf{U}}^{s-1}$.
 - 5: **for** $t = 1, 2, \dots, m_s$ **do**
 - 6: Choose $i_t^s \in \{1, \dots, N\}$ uniformly at random.
 - 7: Calculate the tangent vector ζ from $\tilde{\mathbf{U}}^{s-1}$ to \mathbf{U}_{t-1}^s by logarithm mapping in (3).
 - 8: Calculate the modified Riemannian stochastic gradient ξ_t^s in (9) by parallel-translating $\text{grad}f(\tilde{\mathbf{U}}^{s-1})$ and $\text{grad}f_{i_t^s}(\tilde{\mathbf{U}}^{s-1})$ along ζ in (2) as

$$\xi_t^s = \text{grad}f_{i_t^s}(\mathbf{U}_{t-1}^s) - P_{\gamma}^{\mathbf{U}_{t-1}^s \leftarrow \tilde{\mathbf{U}}^{s-1}} \left(\text{grad}f_{i_t^s}(\tilde{\mathbf{U}}^{s-1}) - \text{grad}f(\tilde{\mathbf{U}}^{s-1}) \right).$$
 - 9: Update \mathbf{U}_t^s from \mathbf{U}_{t-1}^s as $\mathbf{U}_t^s = \text{Exp}_{\mathbf{U}_{t-1}^s}(-\eta\xi_t^s)$ with the exponential mapping (1).
 - 10: **end for**
 - 11: **option I:** $\tilde{\mathbf{U}}^s = g_{m_s}(\mathbf{U}_1^s, \dots, \mathbf{U}_{m_s}^s)$ (or $\tilde{\mathbf{U}}^s = \mathbf{U}_t^s$ for randomly chosen $t \in \{1, \dots, m_s\}$).
 - 12: **option II:** $\tilde{\mathbf{U}}^s = \mathbf{U}_{m_s}^s$.
 - 13: **end for**
-

Additionally, the variants of the variance reduced SGD need full gradient calculation every epoch at the beginning. This poses a bigger overhead than the ordinal SGD algorithm at the beginning of the process, and eventually, this causes *cold-start* property on them. To avoid this, [20] in the Euclidean space proposes to use standard SGD updating only for first epoch. This paper also adopts this simple modification of R-SVRG, denoted as R-SVRG+. We do not analyze this extension and leave this as an open problem.

As mentioned earlier, each iteration of R-SVRG has double loops to reduce the variance of the modified stochastic gradient ξ_t^s . s -th epoch, i.e., outer loop, requires $N + 2m_s$ gradient evaluations, where N is for the full gradient $\text{grad}f(\tilde{\mathbf{U}}^{s-1})$ at the beginning of each s -th epoch and $2m_s$ is for inner iterations since each inner step needs two gradient evaluations, i.e., $\text{grad}f_{i_t^s}(\mathbf{U}_{t-1}^s)$ and $\text{grad}f_{i_t^s}(\tilde{\mathbf{U}}^{s-1})$. However, if $\text{grad}f_{i_t^s}(\tilde{\mathbf{U}}^{s-1})$ for each sample are stored at the beginning of s -th epoch like SAG, the evaluations for each inner loop result in m_s . Finally, s -th epoch requires $N + m_s$ evaluations. It is natural to choose m_s to be the same order of N , but slightly larger (for example $m_s = 5N$ for non-convex problems is suggested in [1]).

4 Main result: convergence analysis

In this section, we provide the results of our convergence analysis. The actual proofs of all the theorems and lemmas are given in the supplementary material.

We first introduce a global convergence result under a *decay step-size* below.

Theorem 4.1. *Consider **Algorithm 1** on a connected Riemannian manifold \mathcal{M} with injectivity radius uniformly bounded from below by $I > 0$. Assume that the sequence of step-sizes $(\eta_t^s)_{m_s \geq t \geq 1, s \geq 1}$ satisfies the condition that $\sum (\eta_t^s)^2 < \infty$ and $\sum \eta_t^s = +\infty$. Suppose there exists a compact set K such that $w_t^s \in K$ for all $t \geq 0$. We also suppose that the gradient is bounded on K , i.e., there exists $A > 0$ such that for all $w \in K$ and $n \in \{1, 2, \dots, n\}$, we have $\|\text{grad}f(w)\| \leq A/3$ and $\|\text{grad}f_n(w)\| \leq A/3$. Then $f(w_t^s)$ converges a.s. and $\text{grad}f(w_t^s) \rightarrow 0$ a.s.*

Proof. Note that $\xi_t^s \leq A$ from the triangle inequality. The proof is done by bounding above the expectation of $f(w_{t+1}^s) - f(w_t^s)$ and $\|\text{grad}f(w_{t+1}^s)\|^2 - \|\text{grad}f(w_t^s)\|^2$. See **Theorem B.2** for details of the proof. \square

Then, we show a local convergence rate analysis. For this purpose, we first show a lemma that upper bounds the variance of ξ_t^s . Subsequently, the local convergence rate theorem for R-SVRG in **Algorithm 1** is given. It should be also noted that the lemma and theorem in this section hold for any compact manifold. In addition, this analysis holds under a *fixed step-size* setup. Here, we assume throughout the following analysis that the functions f_n are β -Lipschitz continuously differentiable (See **Assumption 1** in Section C).

Lemma 4.2. *Let $\mathbb{E}_{i_t^s}[\cdot]$ be the expectation with respect to the random choice of i_t^s , i.e., the expectation is conditioned on all randomness introduced up to the t -th iteration of the inner loop during s -th epoch. When each $\text{grad}f_n$ is β -Lipschitz continuously differentiable, the upper bound of the variance of ξ_t^s is given by*

$$\mathbb{E}_{i_t^s}[\|\xi_t^s\|^2] \leq \beta^2(14(\text{dist}(w_{t-1}^s, w^*))^2 + 8\text{dist}(\tilde{w}^{s-1}, w^*))^2).$$

Proof. The proof is analogous to that of SVRG algorithm in the Euclidean space. However, the distance evaluations of points should be done appropriately on the corresponding same tangent space using parallel translation. The actual proof is in **Lemma C.3** of the supplementary material file. \square

Lemma 4.2 implies that the variance of ξ_t^s converges to zero when both \mathbf{U}_t^s and $\tilde{\mathbf{U}}^{s-1}$ converge to \mathbf{U}^* . Finally, we provide the main theorem of this paper for the local convergence rate of R-SVRG.

Theorem 4.3. *Let \mathcal{M} be the Grassmann manifold and $\mathbf{U}^* \in \mathcal{M}$ be a non-degenerate local minimizer of f (i.e., $\text{grad}f(\mathbf{U}^*) = 0$ and the Hessian $\text{Hess}f(\mathbf{U}^*)$ of f at \mathbf{U}^* is positive definite). Assume that there exists a convex neighborhood \mathcal{U} of $\mathbf{U}^* \in \mathcal{M}$ and a positive real number σ such that the smallest eigenvalue of the Hessian of f at each $\mathbf{U} \in \mathcal{U}$ is not less than σ . When each $\text{grad}f_n$ is β -Lipschitz continuously differentiable and $\eta > 0$ is sufficiently small such that $0 < \eta(\sigma - 14\eta\beta^2) < 1$, it then follows that for any sequence $\{\tilde{\mathbf{U}}^s\}$ generated by the algorithm converging to \mathbf{U}^* , there exists $K > 0$ such that for all $s > K$,*

$$\mathbb{E}[(\text{dist}(\tilde{\mathbf{U}}^s, \mathbf{U}^*))^2] \leq \frac{4(1 + 8m\eta^2\beta^2)}{\eta m(\sigma - 14\eta\beta^2)} \mathbb{E}[(\text{dist}(\tilde{\mathbf{U}}^{s-1}, \mathbf{U}^*))^2].$$

Proof. The proof starts with bounding above the expectation of the distance between \mathbf{U}_t^s and \mathbf{U}^* with respect to the random choice of i_t^s , where the curvature of the Grassmann manifold and **Lemma 6** in [21], which corresponds to the law of cosines in the Euclidean space, are fully used. See **Theorem C.5** for the complete proof. \square

5 Numerical comparisons

This section compares the performance of R-SVRG(+) with the Riemannian extension of SGD, i.e., R-SGD, where the Riemannian stochastic gradient algorithm is $\text{grad}f_{i_t^s}(\mathbf{U}_{t-1}^s)$ instead of ξ_t^s

in (9). We also compare with R-SD, which is the Riemannian steepest descent algorithm with the backtracking line search [14, Chapters 4]. We consider both *fixed* step-size as well as *decay* step-size sequences. The decay step-size sequence uses the decay $\eta_k = \eta_0(1 + \eta_0\lambda\lfloor k/m_s \rfloor)^{-1}$ where k is the number of iterations used. We select ten choices of η_0 , and consider three $\lambda = \{10^{-1}, 10^{-2}, 10^{-3}\}$. In addition, since the global convergence needs a decay step-size condition and the local convergence rate analysis holds for a fixed step-size (Section 4), we consider a *hybrid* step-size sequence that follows the decay step-size at less than s_{TH} epoch, and subsequently switches to a fixed step-size. All experiments use $s_{TH} = 5$ in this experiment. $m_s = 5N$ is also fixed by following [1], and batch-size is fixed to 10. In all the figures, the x -axis is the computational cost measured by the number of gradient computations divided by N . Algorithms are initialized randomly and are stopped when either the stochastic gradient norm is below 10^{-8} or the number of iterations exceeds 100. Additional numerical experiments are shown in Section D of the supplementary material file. It should be noted that all results except R-SD are the best-tuned results. All simulations are performed in Matlab on a 2.6 GHz Intel Core i7 machine with 16 GB RAM.

PCA problem (4). We first consider the PCA problem. Figures 1(a)-(c) show the results of the train loss, *optimality gap*, and the norm of gradient, respectively, where $N = 10000$, $d = 20$, and $r = 5$. η_0 is $\{10^{-3}, 2 \times 10^{-3}, \dots, 10^{-2}\}$. The optimality gap evaluates the performance against the minimum loss, which is obtained by the Matlab function `pca`. Figure 1(a) shows the enlarged results of the train loss, where all algorithms of R-SVRG(+) yield better convergence properties. Among the step-size sequences of R-SVRG(+), the hybrid sequence shows the best performance among all. Between R-SVRG and R-SVRG+, the latter shows superior performance for all step-size sequences. For the optimality gap plots in Figure 1(b), the results follow similar trends as those of train loss plots. In Figure 1(c), while the gradient norm of SGD stays at higher values, those of R-SVRG and R-SVRG+ converge to lower values in all cases.

Karcher mean problem (5). We compute the Karcher mean of N number of r -dimensional subspaces in \mathbb{R}^d . Figures 2(a)-(c) show the results of the train loss, the enlarged train loss, and the norm of gradient, respectively, where $N = 1000$, $d = 300$, and $r = 5$. The ten choices of η_0 are $\{0.1, 0.2, \dots, 1.0\}$. R-SVRG(+) outperforms R-SGD, and the final loss of R-SVRG(+) is less than that of R-SD. It should be noted that R-SVRG+ with the fixed and decay step-sizes decreases faster in the beginning, but eventually, R-SVRG converges to lower losses.

Matrix completion problem (7). The proposed algorithms are also compared with Grouse [19], a state-of-the-art stochastic descent algorithm on the Grassmann manifold. We first consider a synthetic dataset with $N = 5000$, $d = 500$ with rank $r = 5$. Algorithms are initialized randomly as suggested in [22]. The ten choices of η_0 are $\{10^{-3}, 2 \times 10^{-3}, \dots, 10^{-2}\}$ for R-SGD and R-SVRG(+) and $\{0.1, 0.2, \dots, 1.0\}$ for Grouse. This instance considers the loss on a test set Γ , which is different from the training set Ω . We also impose an exponential decay of singular values. The ratio of the largest to the lowest singular value is known as the condition number (CN) of the matrix. For example, at rank 10 the singular values with condition number 100 is obtained using the Matlab function `logspace(-2, 0, 10)`. This instance uses CN=5. The over-sampling ratio (OS) is 5, where the OS determines the number of entries that are known. An OS of 5 implies that $5(N + d - r)r$ number of randomly and uniformly selected entries are known a priori out of the total Nd entries. Figures 3(a) and (b) show the results of loss on test set Γ and the norm of gradient, respectively. The results show the superior performance of our proposed algorithms.

Next, we consider the Jester dataset 1 [23] consisting of ratings of 100 jokes by 24983 users. Each rating is a real number between -10 and 10 . We randomly extract two ratings per user as the training set Ω and test set Γ . The algorithms are run by fixing the rank to $r = 5$ with random initialization. η_0 is chosen from $\{10^{-6}, 2 \times 10^{-6}, \dots, 10^{-5}\}$ for SGD and SVRG(+) and $\{10^{-3}, 2 \times 10^{-3}, \dots, 10^{-2}\}$ for Grouse. Figures 3(c) and (d) show the superior performance of R-SVRG(+) on both the train and test sets.

As a final test, we compare the algorithms on the MovieLens-1M dataset, which is downloaded from <http://grouplens.org/datasets/movielens/>. The dataset has a million ratings corresponding to 6040 users and 3952 movies. η_0 is chosen from $\{10^{-5}, 2 \times 10^{-5}, \dots, 10^{-4}\}$. Figures 3(e) and (f) show the results on the train and test set of all the algorithms except Grouse, which faces issues with convergence on this dataset. R-SVRG(+) shows much faster convergence speed than others, and R-SVRG is better than R-SVRG+ in terms of the final test loss for all step-size algorithms.

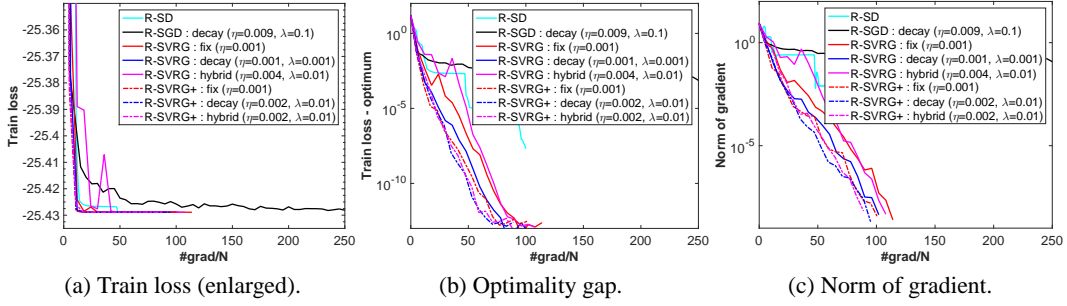


Figure 1: Performance evaluations on PCA problem.

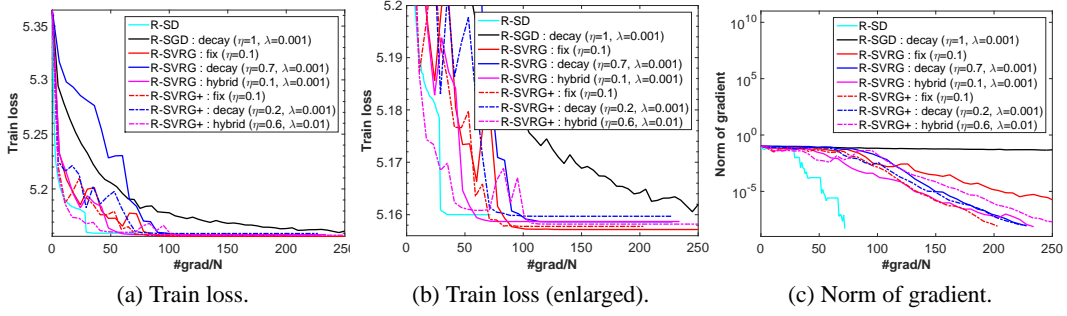


Figure 2: Performance evaluations on Karcher mean problem.

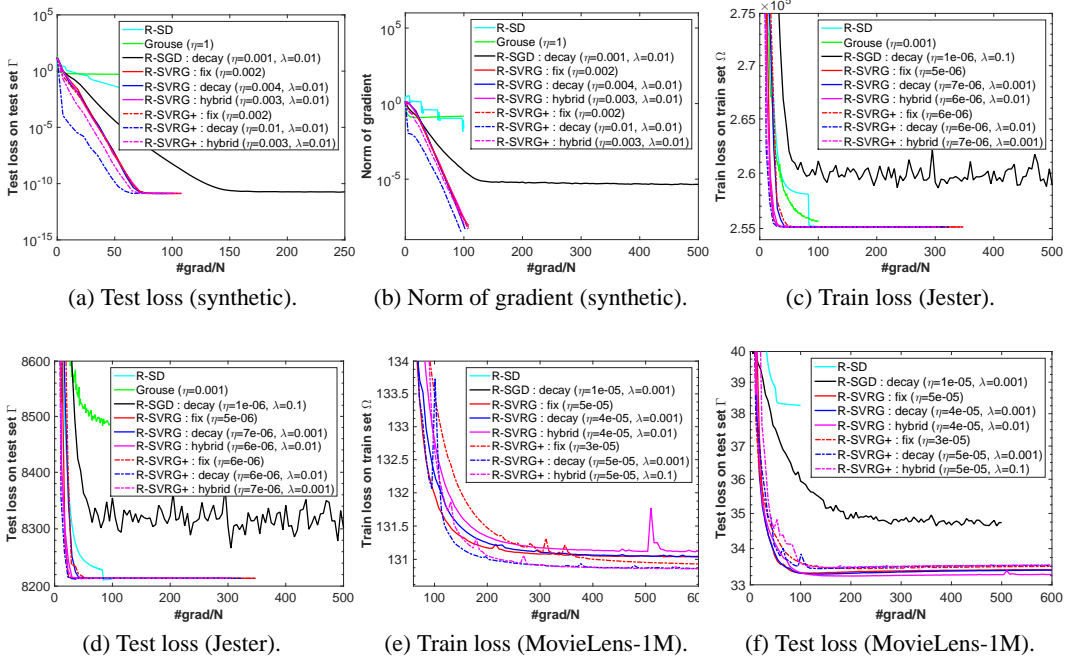


Figure 3: Performance evaluations on low-rank matrix completion problem.

6 Conclusion

We have proposed a Riemannian stochastic variance reduced gradient algorithm (R-SVRG). The proposed algorithm stems from the variance reduced gradient algorithm in the Euclidean space, but is now extended to Riemannian manifolds. The central difficulty of averaging, addition, and subtraction of multiple gradients on a Riemannian manifold is handled with classical notion of parallel

transport. We proved that R-SVRG generates globally convergent sequences with a decay step-size condition and is locally linearly convergent with a fixed step-size under some natural assumptions. We have shown the developments on the Grassmann manifold. Numerical comparisons on three popular problems on the Grassmann manifold suggested the superior performance of R-SVRG on various different benchmarks.

References

- [1] R. Johnson and T. Zhang. Accelerating stochastic gradient descent using predictive variance reduction. In *NIPS*, pages 315–323, 2013.
- [2] Julien Mairal. Incremental majorization-minimization optimization with application to largescale machine learning. *SIAM J. Optim.*, 25(2):829–855, 2015.
- [3] N. L. Roux, M. Schmidt, and F. R. Bach. A stochastic gradient method with an exponential convergence rate for finite training sets. In *NIPS*, pages 2663–2671, 2012.
- [4] S. Shalev-Shwartz and T. Zhang. Proximal stochastic dual coordinate ascent. Technical report, arXiv preprint arXiv:1211.2717, 2012.
- [5] S. Shalev-Shwartz and T. Zhang. Stochastic dual coordinate ascent methods for regularized loss minimization. *JMRL*, 14:567–599, 2013.
- [6] A. Defazio, F. Bach, and S. Lacoste-Julien. SAGA: A fast incremental gradient method with support for non-strongly convex composite objectives. In *NIPS*, 2014.
- [7] Y. Zhang and L. Xiao. Stochastic primal-dual coordinate method for regularized empirical risk minimization. *SIAM J. Optim.*, 24(4):2057–2075, 2014.
- [8] D. Garber and E. Hazan. Fast and simple PCA via convex optimization. Technical report, arXiv preprint arXiv:1509.05647, 2015.
- [9] S. Shalev-Shwartz. SDCA without duality. Technical report, arXiv preprint arXiv:1502.06177, 2015.
- [10] Z. Allen-Zhu and Y. Yan. Improved SVRG for non-strongly-convex or sum-of-non-convex objectives. Technical report, arXiv preprint arXiv:1506.01972, 2015.
- [11] O. Shamir. Fast stochastic algorithms for SVD and PCA: Convergence properties and convexity. Technical report, arXiv preprint arXiv:1507.08788, 2015.
- [12] Z. Allen-Zhu and E. Hazan. Variance reduction for faster non-convex optimization. Technical report, arXiv preprint arXiv:1603.05643, 2016.
- [13] B. Mishra and R. Sepulchre. R3MC: A Riemannian three-factor algorithm for low-rank matrix completion. In *IEEE CDC*, pages 1137–1142, 2014.
- [14] P.-A. Absil, R. Mahony, and R. Sepulchre. *Optimization Algorithms on Matrix Manifolds*. Princeton University Press, 2008.
- [15] S. Bonnabel. Stochastic gradient descent on Riemannian manifolds. *IEEE Trans. on Automatic Control*, 58(9):2217–2229, 2013.
- [16] N. Boumal, B. Mishra, P.-A. Absil, and R. Sepulchre. Manopt: a Matlab toolbox for optimization on manifolds. *JMLR*, 15(1):1455–1459, 2014.
- [17] H Karcher. Riemannian center of mass and mollifier smoothing. *Comm. Pure Appl. Math.*, 30(5):509–541, 1977.
- [18] S. Jayasumana, R. Hartley, M. Salzmann, H. Li, and M. Harandi. Kernel methods on riemannian manifolds with gaussian rbf kernels. *IEEE Trans. Pattern Anal. Mach. Intell.*, 37(12):2464 – 2477, 2015.
- [19] L. Balzano, R. Nowak, and B. Recht. Online identification and tracking of subspaces from highly incomplete information. In *Allerton*, pages 704–711, 2010.
- [20] J. Konečný and P. Richtárik. Semi-stochastic gradient descent methods. Technical report, arXiv preprint arXiv:1312.1666, 2013.
- [21] H. Zhang and S. Sra. First-order methods for geodesically convex optimization. In *COLT*, 2016.
- [22] D. Kressner, M. Steinlechner, and B. Vandereycken. Low-rank tensor completion by Riemannian optimization. *BIT Numer. Math.*, 54(2):447–468, 2014.
- [23] K. Goldberg, T. Roeder, D. Gupta, and C. Perkins. Eigentaste: A constant time collaborative filtering algorithm. *Inform. Retrieval*, 4(2):133–151, 2001.
- [24] B. Mishra and R. Sepulchre. Riemannian preconditioning. *SIAM J. Optim.*, 635–660, 2016.
- [25] G. Meyer, S. Bonnabel, and R. Sepulchre. Linear regression under fixed-rank constraints: A Riemannian approach. In *ICML*, 2011.

- [26] D. L. Fisk. Quasi-martingales. *Trans. Amer. Math. Soc.*, 120(3), 1965.
- [27] R. Tron, B. Afsari, and R. Vidal. Riemannian consensus for manifolds with bounded curvature. *IEEE Transactions on Automatic Control*, 58(4):921–934, 2013.
- [28] K. Shiohama. *An Introduction to the Geometry of Alexandrov Spaces*, volume 8. Seoul National University, Research Institute of Mathematics, Global Analysis Research Center, 1993.

Supplementary material

A Optimization on manifolds

Optimization on manifolds, or *Riemannian optimization*, seeks an optimum (global or local) of a real-valued function defined over a smooth manifold \mathcal{M} . One of the advantages of using Riemannian geometry tools is that constrained optimization problems can be handled as unconstrained optimization problems considering the intrinsic properties of the manifold. This section gives an introductory overview of optimization on manifolds by summarizing the exposition of [14], and the many references therein for more details. We also refer to [24, 25].

Let $f : \mathcal{M} \rightarrow \mathbb{R}$ be a smooth real-valued function on the manifold \mathcal{M} . Computing minimizers of f is our goal. The methods we are interested in for solving this minimization problem are *iterative algorithms* on the manifold \mathcal{M} . Given a starting point $w_0 \in \mathcal{M}$, such iterative algorithms produce a sequence $(w_t)_{t \geq 0}$ in \mathcal{M} that converges to w^* whenever w_0 is in a certain neighborhood, or basin of attraction, of w^* . An iterative optimization algorithm involves computing a search direction and then “moving in that direction.” More concretely, an iteration on a manifold \mathcal{M} is performed by following geodesics (paths of shortest length on the manifold) starting from w_t and tangent to ξ_{w_t} .

$$w_{t+1} = \text{Exp}_{w_t}(s_t \xi_{w_t}),$$

where the search direction ξ_t is in $T_{w_t}\mathcal{M}$ at w_t . The scalar $s_t > 0$ is the step-size. $\text{Exp}_{w_t}(\cdot)$ is the *exponential mapping* [14, Section 5.4] which induces a line-search algorithm along geodesics.

Riemannian gradient. When the search direction ξ_{w_t} considers with $-\text{grad}f(w_t)$, a gradient descent algorithm to minimize f on the manifold is obtained. This $\text{grad}f(w_t)$ is *Riemannian gradient* of f at w_t that is computed according to the chosen metric g at $x \in \mathcal{M}$. This metric is called *Riemannian metric* $g_w : T_w\mathcal{M} \times T_w\mathcal{M} \rightarrow \mathbb{R}$ at $x \in \mathcal{M}$. $g_w(\xi_w, \zeta_w)$ is an inner product between elements ξ_w, ζ_w of the tangent space $T_w\mathcal{M}$ at w . It is defined as the unique element $\text{grad}f(w) \in T_w\mathcal{M}$ that satisfies

$$\text{Df}(w)[\xi_w] = g_w(\text{grad}f(w), \xi_w), \quad \forall \xi_w \in T_w\mathcal{M},$$

where $\text{Df}(w)[\xi_w]$ is the *directional derivative* of $f(w)$ in the direction ξ_w .

Retraction. The geodesics are generally either expensive to compute or not available in closed-form. A more general update formula is obtained below if we relax the constraint of moving along geodesics,

$$w_{t+1} = R_{w_t}(s_t \xi_{w_t}),$$

where R_{w_t} is the *retraction*, which is any map $R_w : T_w\mathcal{M} \rightarrow \mathcal{M}$ that locally approximates the exponential mapping, up to first order, on the manifold [14, Definition 4.1.1]. It provides an attractive alternative to the exponential mapping in the design of optimization algorithms on manifolds, as it reduces the computational cost of the update while retaining the main properties that ensure convergence results.

Quotient manifold. A *quotient manifold* is a set of *equivalence classes*. A simple example is the Grassmann manifold $\text{Gr}(r, d)$, the set of r -dimensional subspaces in \mathbb{R}^d , regarded as a set of r -dimensional orthogonal frames that cannot be superposed by a rotation. For a quotient manifold \mathcal{M}/\sim , where \mathcal{M} is the total space and \sim is the equivalence relation of the form $[w] = \{z \in \mathcal{M} : z \sim w\}$ that defines the quotient, a tangent vector $\xi_{[w]} \in T_{[w]}\mathcal{M}$ at $[w]$ is restricted to the directions that do not induce a displacement along the set of equivalence classes $[w]$. This is realized by decomposing $T_w\mathcal{M}$ into complementary subspaces, the vertical and horizontal subspaces, such that $\mathcal{V}_w \oplus \mathcal{H}_w = T_w\mathcal{M}$. The *vertical space* \mathcal{V}_w is the tangent space of the equivalence class $[w]$. On the other hand, the *horizontal space* \mathcal{H}_w , which is any complementary subspace to \mathcal{V}_w in $T_w\mathcal{M}$, provides a valid matrix representation of the abstract tangent space $T_{[w]}(\mathcal{M}/\sim)$ [14, Section 3.5.8]. This allows us to represent tangent vectors to the quotient space. Indeed, with such a decomposition of $T_{[w]}\mathcal{M}$, a given tangent vector $\xi_{[w]} \in T_{[w]}\mathcal{M}$ at $[w]$ is uniquely represented by a tangent vector $\xi_w \in \mathcal{H}_w$ that satisfies

$$\text{D}\pi(w)[\xi_w] = \xi_{[w]}.$$

The mapping π is the *quotient map* $\pi : w \mapsto [w]$. The tangent vector ξ_w is called the *horizontal lift* of $\xi_{[w]}$ at $[w]$. Provided that the metric $g_w(\xi_w, \eta_w)$ in the total space is invariant along equivalence classes, it defines a metric on the quotient

$$g_{[w]}(\xi_{[w]}, \eta_{[w]}) := g_w(\xi_w, \eta_w).$$

The choice of the metric, which is invariant along the equivalence class $[w]$, and of the horizontal space \mathcal{H}_w as the orthogonal complement of \mathcal{V}_w , in the sense of the Riemannian metric, makes the space \mathcal{M}/\sim a *Riemannian*

submersion. It allows for a convenient matrix representation of the gradient of a cost function. Consequently, the descent algorithm on the manifold \mathcal{M} respects the equivalence property \sim on the space.

Riemannian gradient on quotient manifold. The horizontal lift of the Riemannian gradient $\text{grad}_{[w]}f$ of a cost function, say $f : \mathcal{M} \rightarrow \mathbb{R}$, on the quotient manifold \mathcal{M}/\sim is uniquely represented by the matrix representation, i.e., the

$$\text{horizontal lift of } \text{grad}_{[w]}f = \text{grad}_w f,$$

where $\text{grad}_w f$ is the gradient of f on the computational space \mathcal{M} at w . The equality above is possible due to the invariance of the cost function along the equivalence class $[w]$, the choice of the Riemannian metric, and the choice of the horizontal space \mathcal{H}_w as the orthogonal complement of the vertical space \mathcal{V}_w [14, Section 3.6.2].

Retraction on quotient manifold. The retraction R_w defines a retraction $R_{[w]}(\xi_{[w]}) := [R_w(\xi_w)]$ on the Riemannian quotient manifold \mathcal{M}/\sim , provided that the equivalence class $[R_w(\xi_w)]$ does not depend on the specific choice of the matrix representations of $[w]$ and $\xi_{[w]}$. Here ξ_w is the horizontal lift of an abstract tangent vector $\xi_{[w]} \in T_{[w]}(\mathcal{M}/\sim)$ in \mathcal{H}_w and $[\cdot]$ is the equivalence class defined earlier in the section. Equivalently, the retraction operation $R_{[w]}(\xi_{[w]}) := [R_w(\xi_w)]$ is well defined on \mathcal{M}/\sim when $R_w(\xi_w)$ and $R_z(\xi_z)$ belong to the same equivalence class, i.e., $[R_w(\xi_w)] = [R_z(\xi_z)]$ for all $w, z \in [w]$.

B Global convergence analysis

We assume that the sequence of step-sizes $(\eta_t^s)_{t \geq 1, s \geq 1}$ satisfies the usual condition in stochastic approximation:

$$\sum (\eta_t^s)^2 < \infty \quad \text{and} \quad \sum \eta_t^s = +\infty. \quad (\text{A.1})$$

We also note the following proposition.

Proposition B.1 ([26]). *Let $(X_n)_{n \in \mathbb{N}}$ be a non-negative stochastic process with bounded positive variations, i.e., such that $\sum_0^\infty \mathbb{E}(\mathbb{E}(X_{n+1} - X_n | \mathcal{F}_n)^+) < \infty$. Then the process is a quasi-martingale, i.e.,*

$$\sum_{n=0}^{\infty} \mathbb{E}[X_{n+1} - X_n | \mathcal{F}_n] < \infty \quad \text{a.s.}, \quad \text{and } X_n \text{ converges a.s.}$$

Now, we give the a.s. convergence of the proposed algorithm under some assumptions when the trajectories are guaranteed to remain in a compact set. This is the case if \mathcal{M} is compact, especially if \mathcal{M} is the Grassmann manifold.

Theorem B.2. *Consider Algorithm 1 on a connected Riemannian manifold \mathcal{M} with injectivity radius uniformly bounded from below by $I > 0$. Assume that the sequence of step-sizes $(\eta_t^s)_{m_s \geq t \geq 1, s \geq 1}$ satisfies the condition (A.1). Suppose there exists a compact set K such that $w_t^s \in K$ for all $t \geq 0$. We also suppose that the gradient is bounded on K , i.e., there exists $A > 0$ such that for all $w \in K$ and $n \in \{1, 2, \dots, n\}$, we have $\|\text{grad}f(w)\| \leq A/3$ and $\|\text{grad}f_n(w)\| \leq A/3$. Then $f(w_t^s)$ converges a.s. and $\text{grad}f(w_t^s) \rightarrow 0$ a.s.*

Proof. The claim is proved similarly to the proof of the standard Riemannian SGD (see [15]). Since K is compact, all continuous functions on K can be bounded. Moreover, as $\eta_t^s \rightarrow 0$, there exists t_0 such that for $t \geq t_0$ we have $\eta_t^s A < I$. Suppose now that $t \geq t_0$. It follows from the triangle inequality that $\|\xi_{t+1}^s\| \leq A$, and hence there exists a geodesic $\text{Exp}(-\alpha \eta_t^s \xi_{t+1}^s)_{0 \leq \alpha \leq 1}$ linking w_t^s and w_{t+1}^s as $\text{dist}(w_t^s, w_{t+1}^s) < I$, where ξ_t^s is defined and bounded below

$$\begin{aligned} \xi_t^s &= \text{grad}f_{i_t^s}(w_{t-1}^s) - P_\gamma^{w_{t-1}^s \leftarrow \tilde{w}^{s-1}}(\text{grad}f_{i_t^s}(\tilde{w}^{s-1})) + P_\gamma^{w_{t-1}^s \leftarrow \tilde{w}^{s-1}}(\text{grad}f(\tilde{w}^{s-1})) \\ &\leq A/3 + A/3 + A/3 = A. \end{aligned}$$

$f(\text{Exp}(-\eta_t^s \xi_{t+1}^s)) = f(w_{t+1}^s)$ and thus the Taylor formula implies that

$$f(w_{t+1}^s) - f(w_t^s) \leq -\eta_t^s \langle \xi_{t+1}^s, \text{grad}f(w_t^s) \rangle + (\eta_t^s)^2 \|\xi_{t+1}^s\|^2 k_1,$$

where k_1 is an upper bound of the largest eigenvalues of the Riemannian Hessian of f in the compact set K . Let \mathcal{F}_t^s be the increasing sequence of σ -algebras generated by the variables available just before time t :

$$\mathcal{F}_t^s = \{i_1^1, \dots, i_{m_1}^1, \dots, i_1^{s-1}, \dots, i_{m_{s-1}}^{s-1}, i_1^s, \dots, i_{t-1}^s\}.$$

Since w_t^s is computed from $i_1^s \dots, i_t^s$, it is measurable in \mathcal{F}_{t+1}^s . As i_{t+1}^s is independent from \mathcal{F}_{t+1}^s we have

$$\begin{aligned}
& \mathbb{E}[\langle \xi_{t+1}^s, \text{grad} f(w_t^s) \rangle | \mathcal{F}_{t+1}^s] \\
&= \mathbb{E}_{i_{t+1}^s} [\langle \xi_{t+1}^s, \text{grad} f(w_t^s) \rangle] \\
&= \mathbb{E}[\langle \text{grad} f_{i_{t+1}^s}(w_t^s), \text{grad} f(w_t^s) \rangle | \mathcal{F}_{t+1}^s] \\
&\quad - P_{\gamma}^{w_t^s \leftarrow \tilde{w}^{s-1}} (\mathbb{E}[\langle \text{grad} f_{i_{t+1}^s}(\tilde{w}^{s-1}), \text{grad} f(w_t^s) \rangle | \mathcal{F}_{t+1}^s] - \mathbb{E}[\langle \text{grad} f(\tilde{w}^{s-1}), \text{grad} f(w_t^s) \rangle | \mathcal{F}_{t+1}^s]) \\
&= \mathbb{E}_{i_{t+1}^s} [\langle \text{grad} f_{i_{t+1}^s}(w_t^s), \text{grad} f(w_t^s) \rangle] \\
&\quad - P_{\gamma}^{w_t^s \leftarrow \tilde{w}^{s-1}} (\mathbb{E}_{i_{t+1}^s} [\langle \text{grad} f_{i_{t+1}^s}(\tilde{w}^{s-1}), \text{grad} f(w_{t+1}^s) \rangle] - \langle \text{grad} f(\tilde{w}^{s-1}), \text{grad} f(w_{t+1}^s) \rangle) \\
&= \mathbb{E}_{i_{t+1}^s} [\langle \text{grad} f_{i_{t+1}^s}(w_t^s), \text{grad} f(w_t^s) \rangle] \\
&\quad - P_{\gamma}^{w_t^s \leftarrow \tilde{w}^{s-1}} (\langle \text{grad} f(\tilde{w}^{s-1}), \text{grad} f(w_t^s) \rangle - \langle \text{grad} f(\tilde{w}^{s-1}), \text{grad} f(w_t^s) \rangle) \\
&= \mathbb{E}_{i_{t+1}^s} [\langle \text{grad} f_{i_{t+1}^s}(w_t^s), \text{grad} f(w_t^s) \rangle] \\
&= \|\text{grad} f(w_t^s)\|^2,
\end{aligned}$$

which yields that

$$\mathbb{E}[f(w_{t+1}^s) - f(w_t^s) | \mathcal{F}_{t+1}^s] \leq -\eta_t^s \|\text{grad} f(w_t^s)\|^2 + (\eta_t^s)^2 A^2 k_1, \quad (\text{A.2})$$

as $\|\xi_{t+1}^s\| \leq A$. As $f(w_t^s) \geq 0$, this proves $f(w_t^s) + \sum_{t \geq t_0}^{\infty} (\eta_t^s)^2 A^2 k_1$ is a nonnegative supermartingale, hence it converges a.s. implying that $f(w_t^s)$ converges a.s. Moreover summing the inequalities we have

$$\sum_{t \geq t_0} \eta_t^s \|\text{grad} f(w_t^s)\|^2 \leq - \sum_{t \geq t_0} \mathbb{E}[f(w_{t+1}^s) - f(w_t^s) | \mathcal{F}_t^s] + \sum_{t \geq t_0} (\eta_t^s)^2 A^2 k_1. \quad (\text{A.3})$$

Here we would like to prove the right term is bounded so that the left term converges. But the fact that $f(w_t^s)$ converges does not imply it has bounded variations. However, as in the Euclidian case, we can use a theorem by Fisk [26] ensuring that $f(w_t^s)$ is a quasi martingale, i.e., it can be decomposed into a sum of a martingale and a process whose trajectories are of bounded variation. For a random variable X , let X^+ denote the quantity $\max(X, 0)$.

Summing (A.2) over t , it is clear that $f(w_t^s)$ satisfies the assumption of **Proposition B.1**, and thus $f(w_t^s)$ is a quasi-martingale, implying $\sum_{t \geq t_0} \eta_t^s \|\text{grad} f(w_t^s)\|^2$ converges a.s. because of inequality (A.3) where the central term can be bounded by its absolute value which is convergent thanks to the proposition. But, as $\eta_t^s \rightarrow 0$, this does not prove $\|\text{grad} f(w_t^s)\|$ converges a.s. However, if $\|\text{grad} f(w_t^s)\|$ is proved to converge a.s. it can only converge to 0 a.s. because of condition (A.1).

Now consider the nonnegative process $p_t^s = \|\text{grad} f(w_t^s)\|^2$. Bounding the second derivative of $\|\text{grad} f\|^2$ by k_2 , along the geodesic linking w_t^s and w_{t+1}^s , a Taylor expansion yields

$$p_{t+1}^s - p_t^s \leq -2\eta_t^s \langle \text{grad} f(w_t^s), (\nabla_{w_t^s}^2 f) \xi_{t+1}^s \rangle + (\eta_t^s)^2 \|\xi_{t+1}^s\|^2 k_2,$$

and thus bounding from below the Hessian of f on the compact set by $-k_3$ we have

$$\mathbb{E}(p_{t+1}^s - p_t^s | \mathcal{F}_{t+1}^s) \leq 2\eta_t^s \|\text{grad} f(w_t^s)\|^2 k_3 + (\eta_t^s)^2 A^2 k_2.$$

We just proved the sum of the right term is finite. It implies p_t^s is a quasi-martingale, thus it implies a.s. convergence of p_t towards a value p_t^∞ which can only be 0. \square

C Local convergence rate analysis

We state local convergence properties of the algorithm of R-SVRG: local convergence to local minimizers and its convergence rate.

We first assume throughout the following analysis that the functions f_n are β -Lipschitz continuously differentiable below.

Assumption 1. *We assume that a Riemannian manifold (\mathcal{M}, g) has a positive injectivity radius. A real-valued functions $f_n : \mathcal{M} \rightarrow \mathbb{R}$ are (locally) β -Lipschitz continuously differentiable such that it is differentiable and there exists β such that, for all w, z in \mathcal{M} with $\text{dist}(w, z) < i(\mathcal{M})$. In this case, it holds that [14, Section 7.4.1]*

$$\|P_\alpha^{0 \leftarrow 1} \text{grad} f(z) - \text{grad} f(w)\| \leq \beta \text{dist}(z, w), \quad (\text{A.4})$$

where α is the unique minimizing geodesic with $\alpha(0) = w$ and $\alpha(1) = z$, and $i(\mathcal{M})$ is the injectivity radius which gives a lower bound on the size of the normal neighborhoods. $P_\alpha^{0 \leftarrow 1}(\cdot)$ is a transportation operator from z to w .

Then, we derive the following lemma from the mean-value theorem.

Lemma C.1. *Let f be a cost function on a Riemannian manifold (\mathcal{M}, g) and let w^* be a critical point of f , i.e., $\text{grad}f(w^*) = 0$. Assume that there exists a convex neighborhood \mathcal{U} of $w^* \in \mathcal{M}$ and a positive real number σ such that the smallest eigenvalue of the Hessian of f at each $w \in \mathcal{U}$ is not less than σ . Then,*

$$f(z) \geq f(w) + \langle \text{Exp}_w^{-1}(z), \text{grad}f(w) \rangle_w + \frac{\sigma}{2} \|\text{Exp}_w^{-1}(z)\|_w^2, \quad w, z \in \mathcal{U}$$

Proof. Let $\xi = \text{Exp}_w^{-1}(z)$ for $w, z \in \mathcal{U}$. From our assumption on f and the mean value theorem, we have, for $\lambda \in \mathbb{R}$ sufficiently close to 1,

$$\begin{aligned} f(\text{Exp}_w \lambda \xi) &= f(w) + \lambda \langle \text{grad}f(w), \xi \rangle_w + \lambda^2 \int_0^1 (1-t) \langle \text{Hess}f(\text{Exp}_w t \lambda \xi) [\xi], \xi \rangle_w dt \\ &\geq f(w) + \lambda \langle \text{grad}f(w), \xi \rangle_w + \lambda^2 \sigma \|\xi\|_w^2 \int_0^1 (1-t) dt \\ &= f(w) + \lambda \langle \text{grad}f(w), \xi \rangle_w + \frac{\sigma}{2} \lambda^2 \|\xi\|_w^2. \end{aligned}$$

It follows that

$$f(z) = f(\text{Exp}_w(\xi)) \geq f(w) + \langle \text{grad}f(w), \xi \rangle_w + \frac{\sigma}{2} \|\xi\|_w^2.$$

This completes the proof. \square

Second, we show a property of the Karcher mean on a general Riemannian manifold.

Lemma C.2. *Let w_1, \dots, w_m be points on a Riemannian manifold \mathcal{M} and let w be the Karcher mean of the m points. For an arbitrary point p on \mathcal{M} , we have*

$$(\text{dist}(p, w))^2 \leq \frac{4}{m} \sum_{i=1}^m (\text{dist}(p, w_i))^2.$$

Proof. From the triangle inequality and $(a+b)^2 \leq 2a^2 + 2b^2$ for real numbers a, b , we have for $i = 1, 2, \dots, m$

$$(\text{dist}(p, w))^2 \leq (\text{dist}(p, w_i) + \text{dist}(w_i, w))^2 \leq 2(\text{dist}(p, w_i))^2 + 2(\text{dist}(w_i, w))^2.$$

Since w is the Karcher mean of w_1, w_2, \dots, w_m , it holds that

$$\sum_{i=1}^m (\text{dist}(w, w_i))^2 \leq \sum_{i=1}^m (\text{dist}(p, w_i))^2.$$

It then follows that

$$m \text{dist}(p, w)^2 \leq 2 \sum_{i=1}^m (\text{dist}(p, w_i))^2 + 2 \sum_{i=1}^m (\text{dist}(w_i, w))^2 \leq 4 \sum_{i=1}^m (\text{dist}(p, w_i))^2.$$

This completes the proof. \square

We now derive the upper bound of the variance of ξ_t^s as follows.

Lemma C.3. *Let $\mathbb{E}_{i_t^s}[\cdot]$ be the expectation with respect to the random choice of i_t^s , i.e., the expectation is conditioned on all randomness introduced up to the t -th iteration of the inner loop during s -th epoch. When each $\text{grad}f_n$ is β -Lipschitz continuously differentiable, the upper bound of the variance of ξ_t^s is given by*

$$\mathbb{E}_{i_t^s}[\|\xi_t^s\|^2] \leq \beta^2 (14(\text{dist}(w_{t-1}^s, w^*))^2 + 8\text{dist}(\tilde{w}^{s-1}, w^*))^2. \quad (\text{A.5})$$

Proof. The upper bound of the variance of ξ_t^s in terms of the distance of w_t^s and \tilde{w}^{s-1} from w^* as

$$\begin{aligned}
& \mathbb{E}_{i_t^s} [\|\xi_t^s\|^2] \\
&= \mathbb{E}_{i_t^s} \left[\left\| \left(\text{grad} f_{i_t^s}(w_{t-1}^s) - P_{\gamma}^{w_{t-1}^s \leftarrow w^*} (\text{grad} f_{i_t^s}(w^*)) \right) \right. \right. \\
&\quad \left. \left. + \left(P_{\gamma}^{w_{t-1}^s \leftarrow w^*} (\text{grad} f_{i_t^s}(w^*)) - P_{\gamma}^{w_{t-1}^s \leftarrow \tilde{w}^{s-1}} (\text{grad} f_{i_t^s}(\tilde{w}^{s-1})) + P_{\gamma}^{w_{t-1}^s \leftarrow \tilde{w}^{s-1}} (\text{grad} f(\tilde{w}^{s-1})) \right) \right\|^2 \right] \\
&\leq 2\mathbb{E}_{i_t^s} \left[\left\| \text{grad} f_{i_t^s}(w_{t-1}^s) - P_{\gamma}^{w_{t-1}^s \leftarrow w^*} (\text{grad} f_{i_t^s}(w^*)) \right\|^2 \right] \\
&\quad + 2\mathbb{E}_{i_t^s} \left[\left\| P_{\gamma}^{w_{t-1}^s \leftarrow \tilde{w}^{s-1}} (\text{grad} f_{i_t^s}(\tilde{w}^{s-1})) - P_{\gamma}^{w_{t-1}^s \leftarrow w^*} (\text{grad} f_{i_t^s}(w^*)) - P_{\gamma}^{w_{t-1}^s \leftarrow \tilde{w}^{s-1}} (\text{grad} f(\tilde{w}^{s-1})) \right\|^2 \right] \\
&= 2\mathbb{E}_{i_t^s} \left[\left\| \text{grad} f_{i_t^s}(w_{t-1}^s) - P_{\gamma}^{w_{t-1}^s \leftarrow w^*} (\text{grad} f_{i_t^s}(w^*)) \right\|^2 \right] \\
&\quad + 2\mathbb{E}_{i_t^s} \left[\left\| P_{\gamma}^{w_{t-1}^s \leftarrow \tilde{w}^{s-1}} (\text{grad} f_{i_t^s}(\tilde{w}^{s-1})) - P_{\gamma}^{w_{t-1}^s \leftarrow w^*} (\text{grad} f_{i_t^s}(w^*)) \right\|^2 \right] \\
&\quad - 4 \left\langle P_{\gamma}^{w_{t-1}^s \leftarrow \tilde{w}^{s-1}} (\text{grad} f(\tilde{w}^{s-1})), P_{\gamma}^{w_{t-1}^s \leftarrow \tilde{w}^{s-1}} (\text{grad} f(\tilde{w}^{s-1})) - P_{\gamma}^{w_{t-1}^s \leftarrow w^*} (\text{grad} f(w^*)) \right\rangle \\
&\quad + 2\|P_{\gamma}^{w_{t-1}^s \leftarrow \tilde{w}^{s-1}} (\text{grad} f(\tilde{w}^{s-1}))\|^2 \\
&= 2\mathbb{E}_{i_t^s} \left[\left\| \text{grad} f_{i_t^s}(w_{t-1}^s) - P_{\gamma}^{w_{t-1}^s \leftarrow w^*} (\text{grad} f_{i_t^s}(w^*)) \right\|^2 \right] \\
&\quad + 2\mathbb{E}_{i_t^s} \left[\left\| P_{\gamma}^{w_{t-1}^s \leftarrow \tilde{w}^{s-1}} (\text{grad} f_{i_t^s}(\tilde{w}^{s-1})) - P_{\gamma}^{w_{t-1}^s \leftarrow w^*} (\text{grad} f_{i_t^s}(w^*)) \right\|^2 \right] \\
&\quad - 2\|P_{\gamma}^{w_{t-1}^s \leftarrow \tilde{w}^{s-1}} (\text{grad} f(\tilde{w}^{s-1}))\|^2 \\
&\leq 2\mathbb{E}_{i_t^s} \left[\left\| \text{grad} f_{i_t^s}(w_{t-1}^s) - P_{\gamma}^{w_{t-1}^s \leftarrow w^*} (\text{grad} f_{i_t^s}(w^*)) \right\|^2 \right] \\
&\quad + 2\mathbb{E}_{i_t^s} \left[\left\| P_{\gamma}^{w_{t-1}^s \leftarrow \tilde{w}^{s-1}} (\text{grad} f_{i_t^s}(\tilde{w}^{s-1})) - P_{\gamma}^{w_{t-1}^s \leftarrow w^*} (\text{grad} f_{i_t^s}(w^*)) \right\|^2 \right] \\
&\leq 2\mathbb{E}_{i_t^s} \left[\left\| \text{grad} f_{i_t^s}(w_{t-1}^s) - P_{\gamma}^{w_{t-1}^s \leftarrow w^*} (\text{grad} f_{i_t^s}(w^*)) \right\|^2 \right] \\
&\quad + 2\mathbb{E}_{i_t^s} \left[\left\| P_{\gamma}^{w_{t-1}^s \leftarrow \tilde{w}^{s-1}} (\text{grad} f_{i_t^s}(\tilde{w}^{s-1})) - \text{grad} f_{i_t^s}(w_{t-1}^s) + \text{grad} f_{i_t^s}(w_{t-1}^s) - P_{\gamma}^{w_{t-1}^s \leftarrow w^*} (\text{grad} f_{i_t^s}(w^*)) \right\|^2 \right] \\
&\leq 2\mathbb{E}_{i_t^s} \left[\left\| \text{grad} f_{i_t^s}(w_{t-1}^s) - P_{\gamma}^{w_{t-1}^s \leftarrow w^*} (\text{grad} f_{i_t^s}(w^*)) \right\|^2 \right] \\
&\quad + 4\mathbb{E}_{i_t^s} \left[\left\| P_{\gamma}^{w_{t-1}^s \leftarrow \tilde{w}^{s-1}} (\text{grad} f_{i_t^s}(\tilde{w}^{s-1})) - \text{grad} f_{i_t^s}(w_{t-1}^s) \right\|^2 \right] \\
&\quad + 4\mathbb{E}_{i_t^s} \left[\left\| \text{grad} f_{i_t^s}(w_{t-1}^s) - P_{\gamma}^{w_{t-1}^s \leftarrow w^*} (\text{grad} f_{i_t^s}(w^*)) \right\|^2 \right] \\
&\stackrel{(A.4)}{\leq} \beta^2 (6(\text{dist}(w_{t-1}^s, w^*))^2 + 4(\text{dist}(\tilde{w}^{s-1}, w_{t-1}^s))^2) \\
&\leq \beta^2 (6(\text{dist}(w_{t-1}^s, w^*))^2 + 4(\text{dist}(\tilde{w}^{s-1}, w^*) + \text{dist}(w^*, w_{t-1}^s))^2) \\
&\leq \beta^2 (6(\text{dist}(w_{t-1}^s, w^*))^2 + 8(\text{dist}(\tilde{w}^{s-1}, w^*))^2 + 8(\text{dist}(w^*, w_{t-1}^s))^2) \\
&= \beta^2 (14(\text{dist}(w_{t-1}^s, w^*))^2 + 8(\text{dist}(\tilde{w}^{s-1}, w^*))^2),
\end{aligned}$$

where the first, fourth and seventh inequalities follow from $(a+b)^2 \leq 2a^2 + 2b^2$ for real numbers a, b , and the sixth inequality uses the triangle inequality. The third equality comes from $\mathbb{E}_{i_t^s} [\text{grad} f_{i_t^s}(\tilde{w}^{s-1})] = \text{grad} f(\tilde{w}^{s-1})$, and the fourth equality from $\text{grad} f(w^*) = 0$. \square

Now we introduce **Lemma 6** in [21] to evaluate the distance between x_t^s and x^* using the smoothness of our objective function.

Lemma C.4 (Lemma 6 in [21]). *If a, b, c are the sides (i.e., side lengths) of a geodesic triangle in an Alexandrov space with curvature lower bounded by κ , and A is the angle between sides b and c , then*

$$a^2 \leq \frac{\sqrt{|\kappa|}c}{\tanh(\sqrt{|\kappa|}c)} b^2 + c^2 - 2bc \cos(A).$$

Note that all the theorems and lemmas above hold for the Grassmann manifold. In the last theorem, we consider the Grassmann manifold specifically.

Theorem C.5. *Let \mathcal{M} be the Grassmann manifold and $\mathbf{U}^* \in \mathcal{M}$ be a non-degenerate local minimizer of f (i.e., $\text{grad} f(\mathbf{U}^*) = 0$ and the Hessian $\text{Hess} f(\mathbf{U}^*)$ of f at \mathbf{U}^* is positive definite) and suppose that the assumption in Lemma C.1 holds. When each $\text{grad} f_n$ is β -Lipschitz continuously differentiable and $\eta > 0$ is sufficiently*

small such that $0 < \eta(\sigma - 14\eta\beta^2) < 1$, it then follows that for any sequence $\{\tilde{\mathbf{U}}^s\}$ generated by the algorithm converging to \mathbf{U}^* , there exists $K > 0$ such that for all $s > K$,

$$\mathbb{E}[(\text{dist}(\tilde{\mathbf{U}}^s, \mathbf{U}^*))^2] \leq \frac{4(1 + 8m\eta^2\beta^2)}{\eta m(\sigma - 14\eta\beta^2)} \mathbb{E}[(\text{dist}(\tilde{\mathbf{U}}^{s-1}, \mathbf{U}^*))^2].$$

Proof. The Grassmann manifold is geodesically complete [14] and the sectional curvature of the Grassmann manifold is bounded below by 0 [27]. Every complete Riemannian manifold whose sectional curvature is bounded below is an Alexandrov space [28]. Therefore, the Grassmann manifold satisfies the assumptions in **Lemma C.4** with $\kappa = 0$. Then, conditioned on \mathbf{U}_{t-1}^s , the expectation of the distance between \mathbf{U}_t^s and \mathbf{U}^* with respect to the random choice of i_t^s is evaluated as

$$\begin{aligned} & \mathbb{E}_{i_t^s} [(\text{dist}(\mathbf{U}_t^s, \mathbf{U}^*))^2] \\ & \leq \mathbb{E}_{i_t^s} [(\text{dist}(\mathbf{U}_{t-1}^s, \mathbf{U}_t^s))^2 + (\text{dist}(\mathbf{U}_{t-1}^s, \mathbf{U}^*))^2 - 2\langle \text{Exp}_{\mathbf{U}_{t-1}^s}^{-1}(\mathbf{U}_t^s), \text{Exp}_{\mathbf{U}_{t-1}^s}^{-1}(\mathbf{U}^*) \rangle_{\mathbf{U}_{t-1}^s}]. \end{aligned}$$

It follows that

$$\begin{aligned} & \mathbb{E}_{i_t^s} [(\text{dist}(\mathbf{U}_t^s, \mathbf{U}^*))^2 - (\text{dist}(\mathbf{U}_{t-1}^s, \mathbf{U}^*))^2] \\ & \leq \mathbb{E}_{i_t^s} [(\text{dist}(\mathbf{U}_{t-1}^s, \mathbf{U}_t^s))^2 - 2\langle -\eta\xi_t^s, \text{Exp}_{\mathbf{U}_{t-1}^s}^{-1}(\mathbf{U}^*) \rangle_{\mathbf{U}_{t-1}^s}] \\ & = \mathbb{E}_{i_t^s} [(\text{dist}(\mathbf{U}_{t-1}^s, \mathbf{U}_t^s))^2 + 2\eta\langle \text{grad}f(\mathbf{U}_{t-1}^s), \text{Exp}_{\mathbf{U}_{t-1}^s}^{-1}(\mathbf{U}^*) \rangle_{\mathbf{U}_{t-1}^s}], \end{aligned}$$

where the last equality follows

$$\begin{aligned} \mathbb{E}_{i_t^s} [\xi_t^s] &= \mathbb{E}_{i_t^s} [\text{grad}f_{i_t^s}(\mathbf{U}_{t-1}^s)] - P_\gamma^{\mathbf{U}_{t-1}^s \leftarrow \tilde{\mathbf{U}}^{s-1}} \left(\mathbb{E}_{i_t^s} [\text{grad}f_{i_t^s}(\tilde{\mathbf{U}}^{s-1})] - \text{grad}f(\tilde{\mathbf{U}}^{s-1}) \right) \\ &= \text{grad}f(\mathbf{U}_{t-1}^s) - P_\gamma^{\mathbf{U}_{t-1}^s \leftarrow \tilde{\mathbf{U}}^{s-1}} \left(\text{grad}f(\tilde{\mathbf{U}}^{s-1}) - \text{grad}f(\tilde{\mathbf{U}}^{s-1}) \right) \\ &= \text{grad}f(\mathbf{U}_{t-1}^s). \end{aligned}$$

Lemma C.1 together with the relation $f(\mathbf{U}^*) \leq f(\mathbf{U}_{t-1}^s)$ yields that

$$\langle \text{grad}f(\mathbf{U}_{t-1}^s), \text{Exp}_{\mathbf{U}_{t-1}^s}^{-1}(\mathbf{U}^*) \rangle_{\mathbf{U}_{t-1}^s} \leq -\frac{\sigma}{2} \|\text{Exp}_{\mathbf{U}_{t-1}^s}^{-1}(\mathbf{U}^*)\|_{\mathbf{U}_{t-1}^s}^2 = -\frac{\sigma}{2} (\text{dist}(\mathbf{U}_{t-1}^s, \mathbf{U}^*))^2,$$

with the assumption that K is sufficient large. We thus obtain by **Lemma C.3**

$$\begin{aligned} & \mathbb{E} [(\text{dist}(\mathbf{U}_t^s, \mathbf{U}^*))^2 - (\text{dist}(\mathbf{U}_{t-1}^s, \mathbf{U}^*))^2] \\ & \leq \mathbb{E} [\|\eta\xi_t^s\|^2 - \sigma\eta(\text{dist}(\mathbf{U}_{t-1}^s, \mathbf{U}^*))^2] \\ & \stackrel{(A.5)}{\leq} \eta^2\beta^2\mathbb{E}[14(\text{dist}(\mathbf{U}_{t-1}^s, \mathbf{U}^*))^2 + 8(\text{dist}(\tilde{\mathbf{U}}^{s-1}, \mathbf{U}^*))^2 - \sigma\eta(\text{dist}(\mathbf{U}_{t-1}^s, \mathbf{U}^*))^2] \\ & = \eta(14\eta\beta^2 - \sigma)\mathbb{E}[(\text{dist}(\mathbf{U}_{t-1}^s, \mathbf{U}^*))^2 + 8\eta^2\beta^2(\text{dist}(\tilde{\mathbf{U}}^{s-1}, \mathbf{U}^*))^2]. \end{aligned}$$

It follows that

$$\begin{aligned} & \mathbb{E}_{i_t^s} [(\text{dist}(\mathbf{U}_t^s, \mathbf{U}^*))^2 - (\text{dist}(\mathbf{U}_{t-1}^s, \mathbf{U}^*))^2] \\ & \leq \eta(14\eta\beta^2 - \sigma)\mathbb{E}_{i_t^s} [(\text{dist}(\mathbf{U}_{t-1}^s, \mathbf{U}^*))^2 + 8\eta^2\beta^2(\text{dist}(\tilde{\mathbf{U}}^{s-1}, \mathbf{U}^*))^2]. \end{aligned}$$

Summing over $t = 1, \dots, m$ of the inner loop on s -th epoch, we have

$$\begin{aligned} & \mathbb{E}[(\text{dist}(\mathbf{U}_m^s, \mathbf{U}^*))^2 - (\text{dist}(\mathbf{U}_0^s, \mathbf{U}^*))^2] \\ & \leq \eta(14\eta\beta^2 - \sigma) \sum_{t=1}^m \mathbb{E}[(\text{dist}(\mathbf{U}_{t-1}^s, \mathbf{U}^*))^2] + 8m\eta^2\beta^2(\text{dist}(\tilde{\mathbf{U}}^{s-1}, \mathbf{U}^*))^2. \end{aligned}$$

Rearranging and using $\mathbf{U}_0^s = \tilde{\mathbf{U}}^{s-1}$, we obtain

$$\begin{aligned} & \eta(\sigma - 14\eta\beta^2) \sum_{t=1}^m \mathbb{E}[(\text{dist}(\mathbf{U}_t^s, \mathbf{U}^*))^2] \\ & = \eta(\sigma - 14\eta\beta^2) \mathbb{E} \left[\sum_{t=0}^{m-1} (\text{dist}(\mathbf{U}_t^s, \mathbf{U}^*))^2 + (\text{dist}(\mathbf{U}_m^s, \mathbf{U}^*))^2 - (\text{dist}(\mathbf{U}_0^s, \mathbf{U}^*))^2 \right] \\ & \leq \mathbb{E} [(\text{dist}(\mathbf{U}_0^s, \mathbf{U}^*))^2 - (\text{dist}(\mathbf{U}_m^s, \mathbf{U}^*))^2 + 8m\eta^2\beta^2(\text{dist}(\mathbf{U}_0^s, \mathbf{U}^*))^2 \\ & \quad - \eta(\sigma - 14\eta\beta^2)((\text{dist}(\mathbf{U}_0^s, \mathbf{U}^*))^2 - (\text{dist}(\mathbf{U}_m^s, \mathbf{U}^*))^2)] \\ & \leq (1 - \eta(\sigma - 14\eta\beta^2) + 8m\eta^2\beta^2) \mathbb{E}[(\text{dist}(\mathbf{U}_m^s, \mathbf{U}^*))^2] \\ & \leq (1 + 8m\eta^2\beta^2) \mathbb{E}[(\text{dist}(\tilde{\mathbf{U}}^{s-1}, \mathbf{U}^*))^2]. \end{aligned}$$

Using $\tilde{\mathbf{U}}^s = g_m(\mathbf{U}_1^s, \dots, \mathbf{U}_m^s)$ and **Lemma C.2**, we obtain

$$\mathbb{E}[(\text{dist}(\tilde{\mathbf{U}}^s, \mathbf{U}^*))^2] \leq \frac{4(1 + 8m\eta^2\beta^2)}{\eta m(\sigma - 14\eta\beta^2)} \mathbb{E}[(\text{dist}(\tilde{\mathbf{U}}^{s-1}, \mathbf{U}^*))^2].$$

□

In the above theorem, we note that, from the definitions of β and σ , β can be chosen arbitrarily large and σ arbitrarily small. Therefore, $\eta = \sigma/28\beta^2$, for example, satisfies $0 < \eta(\sigma - 14\eta\beta^2) < 1$ for sufficiently large β and small σ .

D Additional numerical comparison

In addition to the representative numerical comparisons in the paper, we show additional numerical experiments.

PCA problem (additional experiments). We consider the PCA problem of $N = 10000$, $d = 20$, and $r = 10$. Whereas the manuscript provides the results for the case of $r = 5$, here we show the results for the case of $r = 10$. Figure A.1(a) shows the train loss, optimality gap, and the norm of gradient. These results indicate the superior performances of R-SVRG and R-SVRG+. In addition, we consider a larger-scale instance with $d = 100$ and $d = 20$. The results are shown in Figures A.1(b) and A.1(c) for two different ranks $r = 5$ and $r = 10$, respectively. Overall, we find the superior performances of R-SVRG and R-SVRG+.

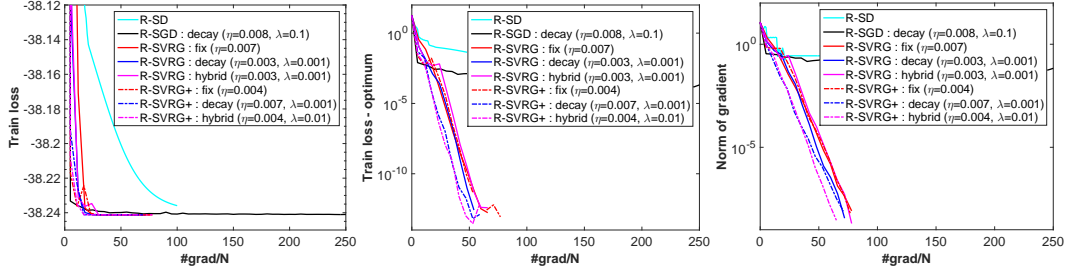
Karcher mean problem (additional experiments). The manuscript shows the results for the case of $r = 5$, where $N = 1000$, $d = 300$, Figure A.2(a) shows the results of $r = 10$. In this instance, R-SVRG+ shows superior performance than R-SVRG in terms of the final loss values. Furthermore, Figures A.2(b) and (c) shows the results for the case with $N = 1000$ and $d = 100$ and with $r = 5$ and $r = 10$, respectively. R-SVRG outperforms R-SGD and the final loss of R-SVRG is less than that of R-SD.

Matrix completion problem (additional experiments). We show the additional results for the smaller instances $N = 1000$, $d = 500$, and $r = 5$ in Figure A.3(a). R-SGD and Grouse decrease very fast in the beginning, but R-SVRG(+) converges to lower values. Figure A.3(b) also shows the case of $r = 10$. Although Grouse indicates the fastest convergence, and gives the lowest values in the train loss as the same R-SVRG(+), R-SVRG(+) outperforms Grouse and R-SGD in test loss. In addition, we show all the results of for $N = 5000$, $d = 500$, and $r = 5$ in Figure A.4(a). These experiments are identical to those in the manuscript. The results show the superior performance of our proposed algorithms. Furthermore, we consider a higher rank of $r = 10$ in Figure A.4(b). The results also show that R-SVRG yield better performances than Grouse and R-SGD.

Next, we show additional results on the Jester dataset 1. We first show all the results in Figure A.5(a) for the case of $r = 5$, some of which are shown in the manuscript. Figure A.5(b) with a larger rank $r = 10$. Overall, our proposed R-SVRG and R-SVRG+ indicate much better convergence than R-SD, R-SGD, and Grouse.

Finally, we show results on the MovieLens-1M dataset. Figure A.6(a) shows the results for the rank 5. Figures A.6(a-2) and (a-4) are identical to those in the manuscript. We also show results with larger rank $r = 10$ case in Figure A.6(b). Once again, our proposed R-SVRG and R-SVRG+ show better results than R-SD and R-SGD.

Effect of batch-size. Here, we show the effect of batch-size on R-SVRG. For this purpose, we consider the PCA problem of $N = 10000$, $d = 20$, and $r = 5$. Figures A.7(a)-(c) show the results for three step-size sequences of R-SVRG, respectively. We consider five different batch-sizes from $\{5, 10, 25, 50, 100\}$. The figures show that R-SVRG similar performance across different batch-sizes.

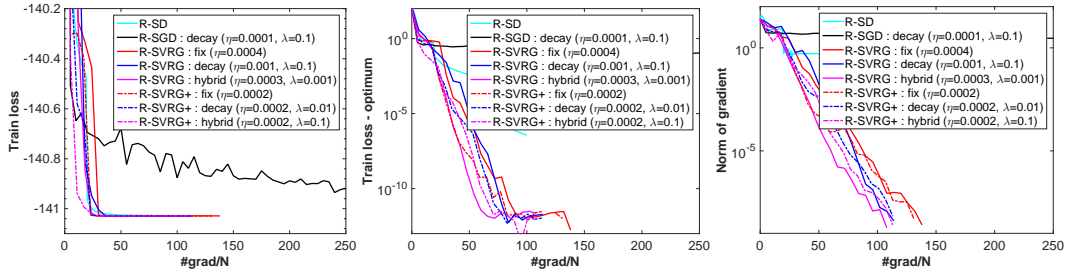


(a-1) Train loss (enlarged).

(a-2) Optimality gap.

(a-3) Norm of gradient.

(a) $N = 10000, d = 20, r = 10$.

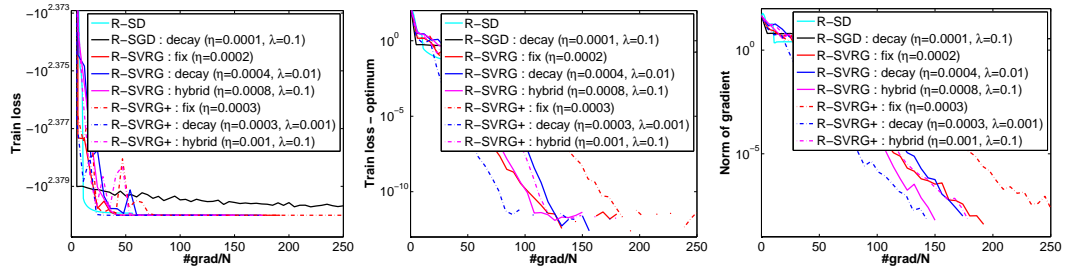


(b-1) Train loss (enlarged).

(b-2) Optimality gap.

(b-3) Norm of gradient.

(b) $N = 10000, d = 100, r = 5$.



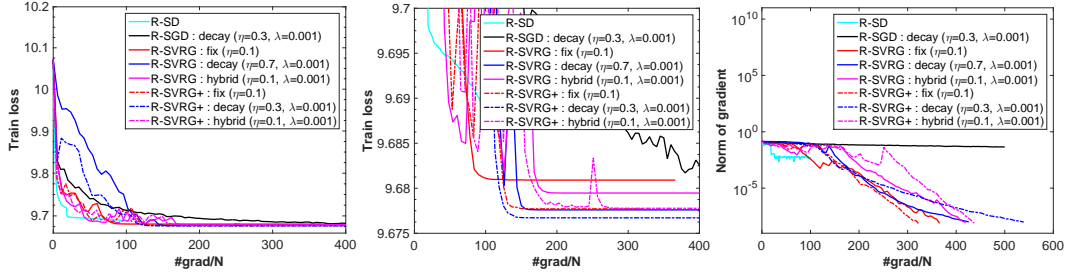
(c-1) Train loss (enlarged).

(c-2) Optimality gap.

(c-3) Norm of gradient.

(c) $N = 10000, d = 100, r = 10$.

Figure A.1: The PCA problem.

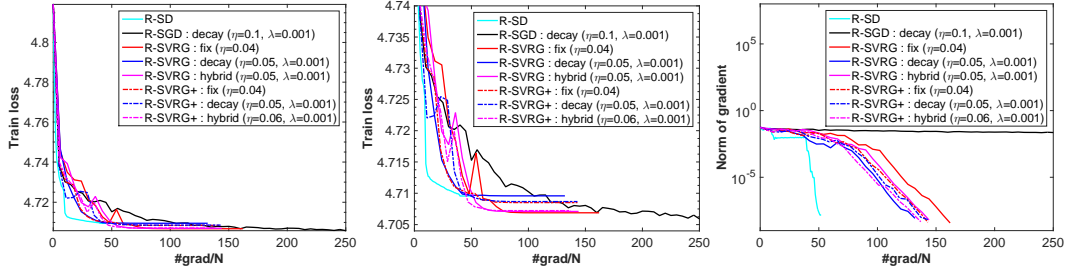


(a-1) Train loss.

(a-2) Train loss (enlarged).

(a-3) Norm of gradient.

(a) $N = 1000, d = 300, r = 10$.

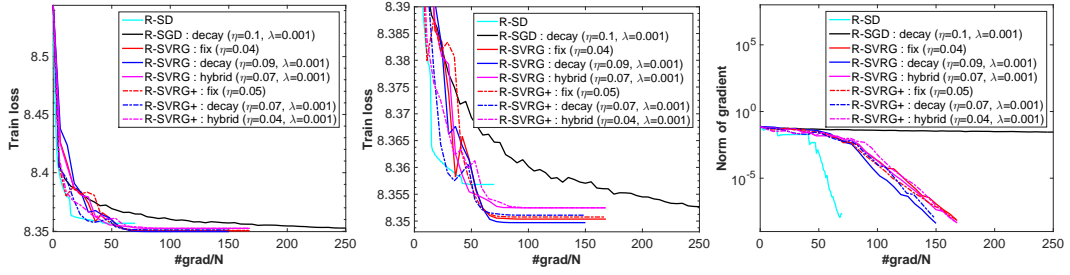


(b-1) Train loss.

(b-2) Train loss (enlarged).

(b-3) Norm of gradient.

(b) $N = 3000, d = 100, r = 5$.



(c-1) Train loss.

(c-2) Train loss (enlarged).

(c-3) Norm of gradient.

(c) $N = 3000, d = 100, r = 10$.

Figure A.2: The Karcher mean problem.

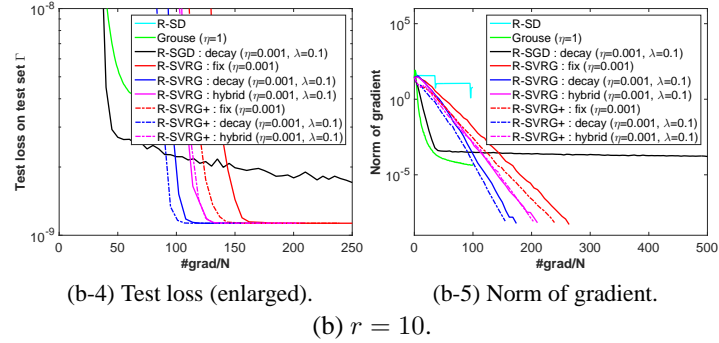
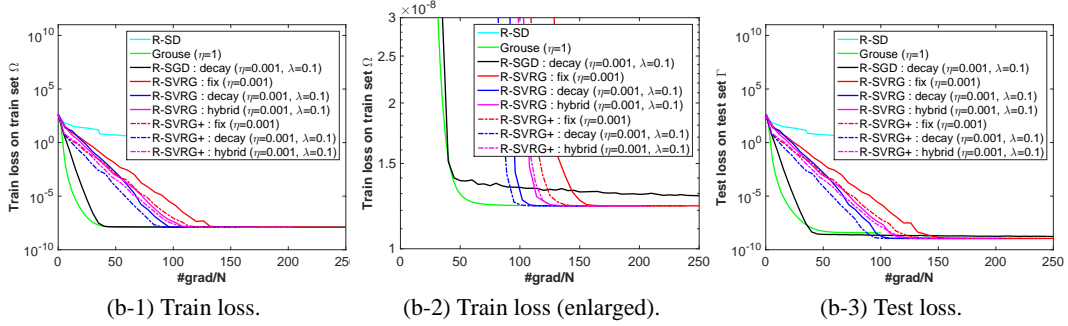
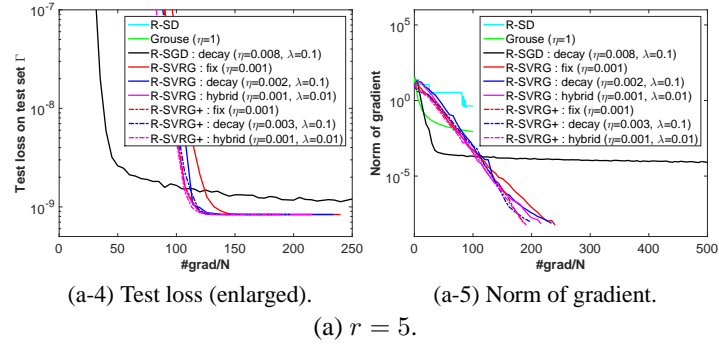
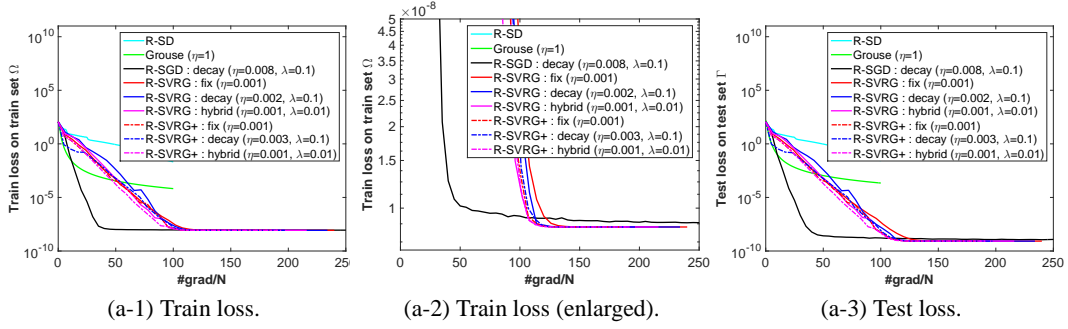


Figure A.3: Low-rank matrix completion problem (synthetic dataset: $N = 1000, d = 500$).

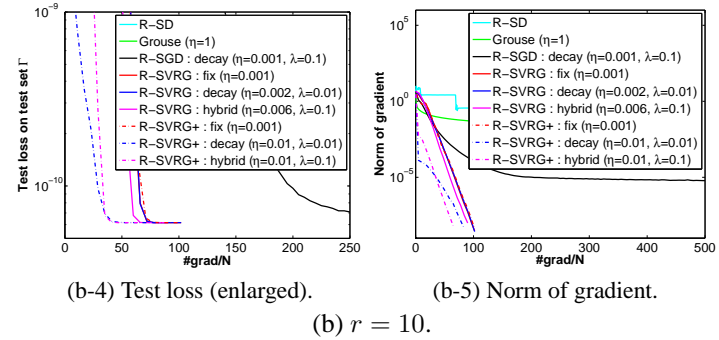
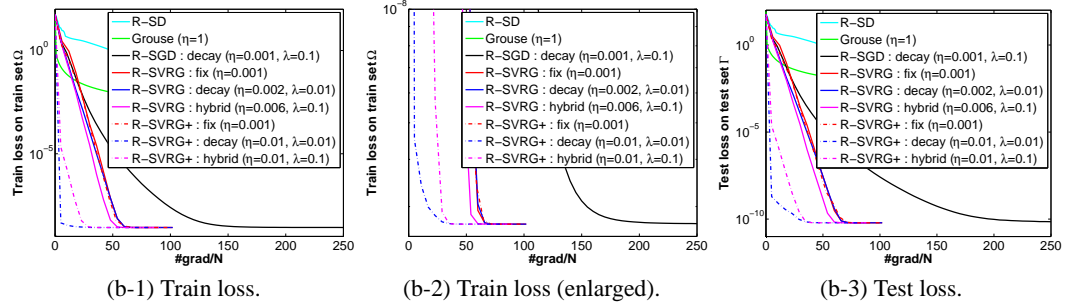
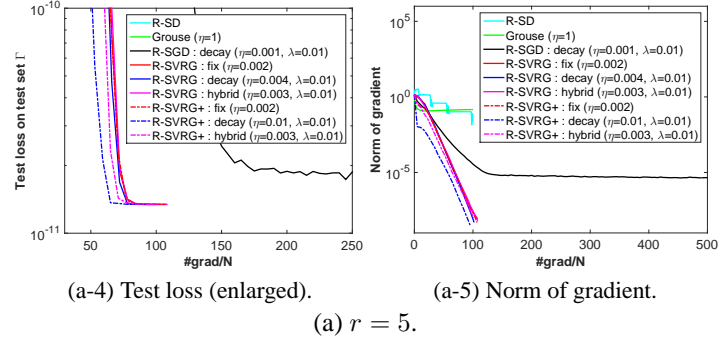
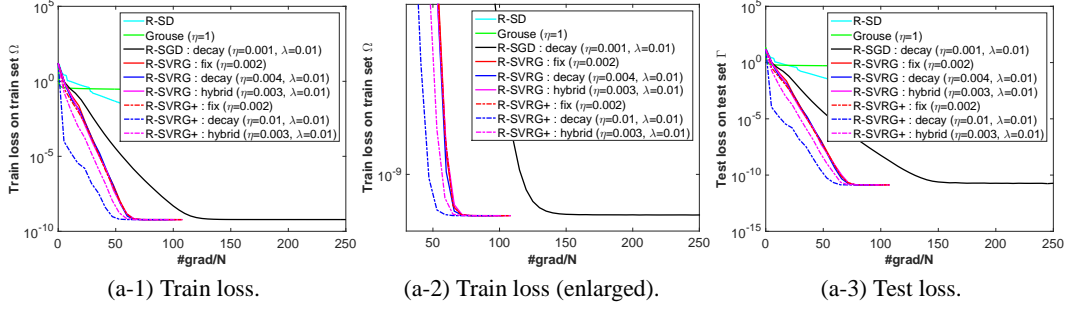
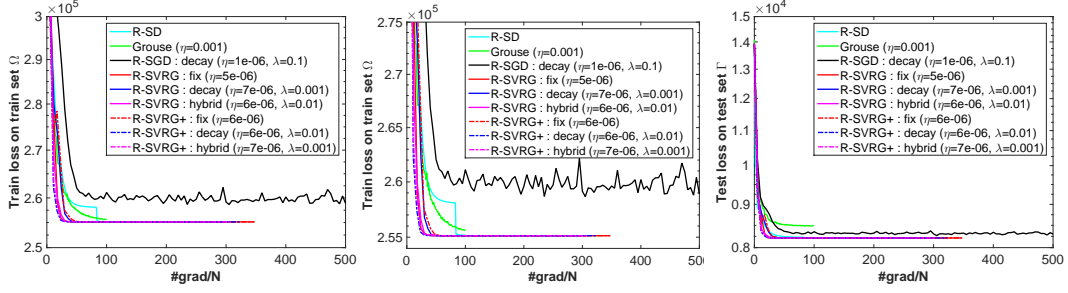


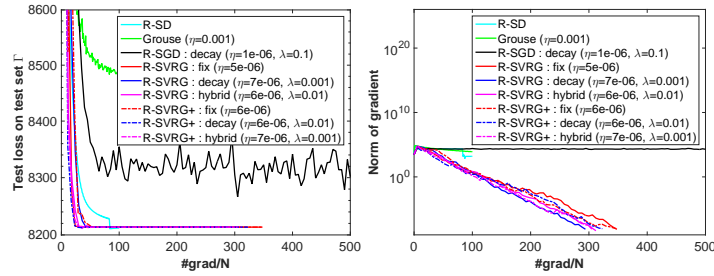
Figure A.4: The low-rank matrix completion problem (synthetic dataset: $N = 5000$, $d = 500$).



(a-1) Train loss.

(a-2) Train loss (enlarged).

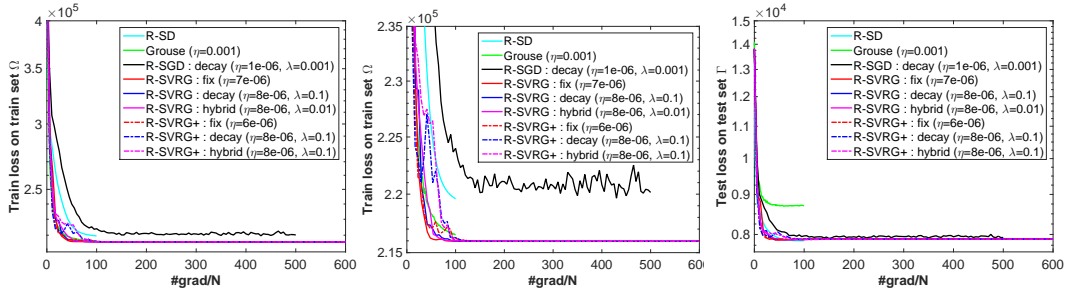
(a-3) Test loss.



(a-4) Test loss (enlarged).

(a-5) Norm of gradient.

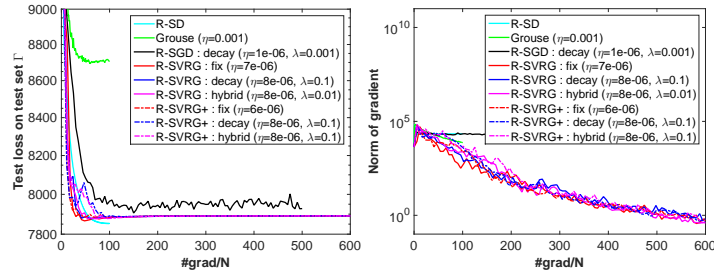
(a) $r = 5$.



(b-1) Train loss.

(b-2) Train loss (enlarged).

(b-3) Test loss.



(b-4) Test loss (enlarged).

(b-5) Norm of gradient.

(b) $r = 10$.

Figure A.5: The low-rank matrix completion problem (Jester dataset).

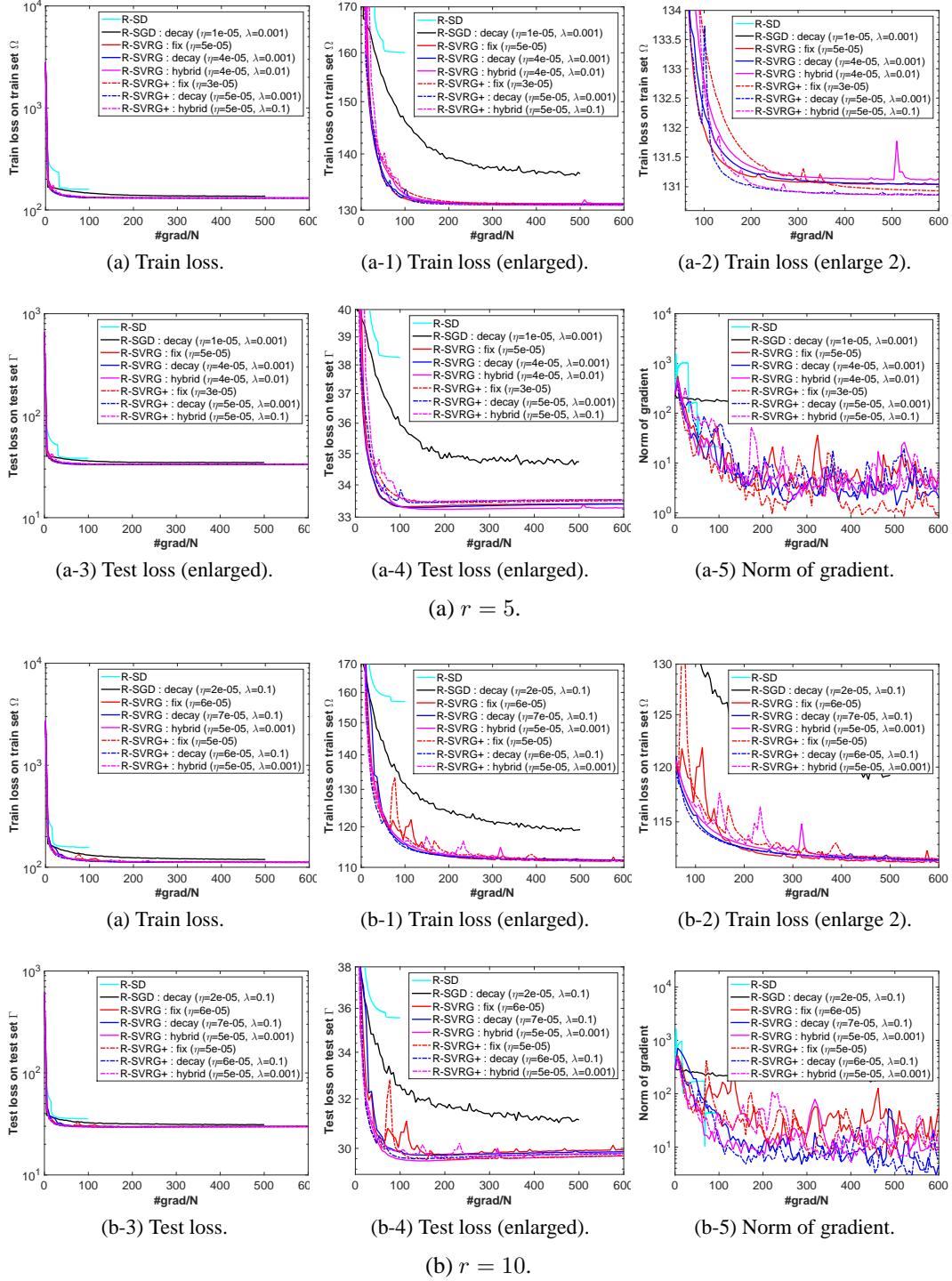
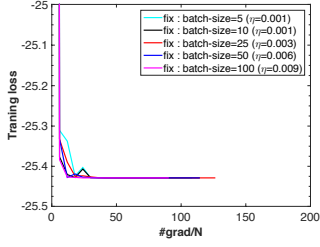
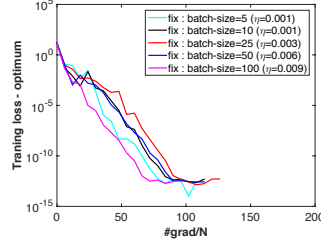


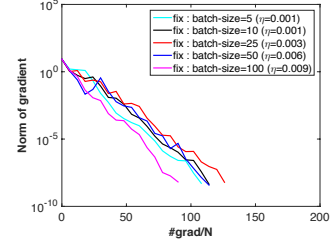
Figure A.6: The low-rank matrix completion problem (MovieLens-1M dataset).



(a-1) Train loss (enlarged).

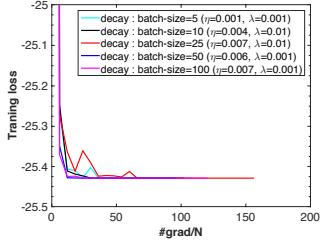


(a-2) Optimality gap.

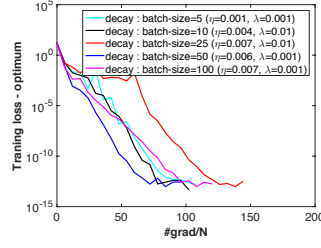


(a-3) Norm of gradient.

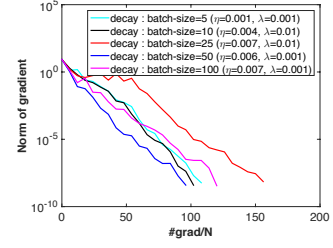
(a) R-SVRG with fixed step-size.



(b-1) Train loss (enlarged).

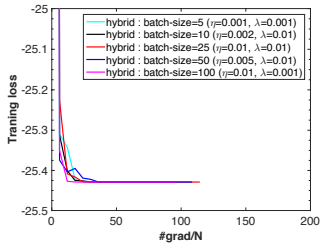


(b-2) Optimality gap.

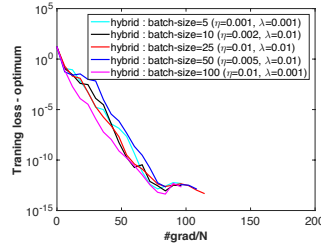


(b-3) Norm of gradient.

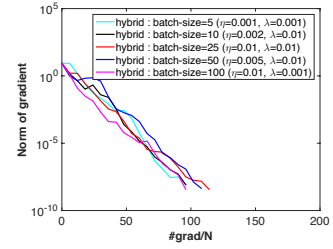
(b) R-SVRG with decay step-size.



(c-1) Train loss (enlarged).



(c-2) Optimality gap.



(c-3) Norm of gradient.

(c) R-SVRG with hybrid step-size.

Figure A.7: Batch-size comparisons for R-SVRG (PCA problem: $N = 10000, d = 20, r = 5$).